OXFORD UNIVERSITY PRESS
IMA Journal of Numerical Analysis

Finite element analysis of a static fluid-solid interaction problem

Journal:	*IMA Journal of Numerical Analysis*
Manuscript ID:	IMAJNA-ES-2009-011.R1
Manuscript Type:	Original Manuscript
Keywords:	fluid-solid interaction, biomechanical brain model, finite elements, a priori and a posteriori error estimates, adaptive scheme

IMA Journal of Numerical Analysis (2005) Page 1 of 27
doi: 10.1093/imanum/dri000

Finite element analysis of a static fluid-solid interaction problem

RODOLFO ARAYA∗
CI²MA, Departamento de Ingeniería Matemática, Universidad de Concepción, Casilla 160-C, Concepción, Chile

GABRIEL R. BARRENECHEA†
Department of Mathematics, University of Strathclyde, 26 Richmond Street Glasgow G1 1XH, Scotland

FABRICE JAILLET‡
Université de Lyon, CNRS UMR 5205, LIRIS - SAARA team, F-69622 Villeurbanne cedex, France

AND

RODOLFO RODRÍGUEZ§
CI²MA, Departamento de Ingeniería Matemática, Universidad de Concepción, Casilla 160-C, Concepción, Chile

This paper deals with a fluid-solid interaction problem inspired by a biomechanical brain model. The problem consists of determining the response to prescribed static forces of an elastic solid containing a barotropic and inviscid fluid at rest. The solid is described by means of displacement variables, whereas displacement potential and pressure are used for the fluid. This approach leads to a well posed symmetric mixed problem, which is discretized by standard Lagrangian finite elements of arbitrary order for all the variables. Optimal order error estimates in H^1 and L^2 norms are proved for this method. A residual a posteriori error estimator is also proposed, for which efficiency and reliability estimates are proved. Finally, some numerical tests are reported to assess the performance of the method and that of an adaptive scheme based on the error estimator.

Keywords: fluid-solid interaction, biomechanical brain model, finite elements, a priori and a posteriori error estimates, adaptive scheme.

1. Introduction

The need for computing fluid-solid interactions arises in many important engineering and biomedical problems. This paper deals with a specific problem of this kind arising from image-guided neurosurgery, which can be seen from the mechanical viewpoint as a static source coupled problem involving an elastic material containing a nearly incompressible fluid.

Current medical imaging devices (magnetic resonance, computed tomography, etc.) facilitate the preoperative planning (see Bucholz *et al.* (1997); Paulsen *et al.* (1999)) and enable the surgeon to locate neuroanatomical structures of interest (see Hill *et al.* (1998); Maurer *et al.* (1998)). However, the

∗Email: raraya@ing-mat.udec.cl
†Email: grb@maths.strath.ac.uk
‡Email: fjaillet@liris.cnrs.fr
§Email: rodolfo@ing-mat.udec.cl

correspondence between preoperatively acquired data and current patient anatomy is typically not very accurate. In fact, it suffers from significant position and shape changes of the brain tissue, usually known as *brain shift*, occurring during neurosurgery (see Bucholz *et al.* (1997); Hill *et al.* (1998)).

In order to predict brain deformation, and thus to correct the preoperatively acquired images according to intraoperative effects, many biomechanical models of the human head have been developed (see, for instance, Fung (1993)). Classical models simulate the mechanical behavior of the different anatomical structures just by varying their physical parameter values (see, for instance, Hagemann *et al.* (1999)). However, such simplification generally leads to non accurate simulations, particularly in case of combined elastic and fluid-filled structures, as it happens, for instance, with the cerebrospinal fluid contained in the brain ventricular system (see Hagemann (2001)).

Recently, Hagemann *et al.* (2002) introduced a biomechanical brain model including fluid-solid interactions, based on linear elasticity for the brain tissue coupled with the Stokes equation for the fluid. Our approach is simpler but, as will be shown below, allows for more efficient solution strategies. We consider a homogeneous fluid at rest, for which its reference density is constant. Therefore, neither viscous effects nor convective terms have to be taken into account. In its turn, since the solid displacements are small, we can suppose a linear response, although some hints about the extension of the analysis to a nonlinear case are also given.

A large amount of work has been devoted during the last years to fluid-solid vibration problems. A survey including several alternative formulations can be found in Bermúdez *et al.* (2008), which include further references. In particular, formulations describing the fluid by means of displacements have been shown to be very efficient for this kind of problems. However, they lead to singular stiffness matrices, unless some irrotational constraint is imposed (see Gastaldi (1996)).

In this paper, we consider a formulation where the fluid is described redundantly by means of two scalar variables, pressure and displacement potential, whereas the standard description in terms of displacements is used for the solid. This leads to a symmetric weak formulation for the coupled problem. One advantage is the possibility of using equal order interpolation spaces for all the variables, without the need to introduce any further unknown in the form of a Lagrange multiplier to treat the transmission conditions. This approach has been originally proposed by Morand & Ohayon (1995) for vibration problems, who named it the *stiffness coupling formulation*, and was analyzed by Bermúdez *et al.* (2003).

The plan of the paper is as follows. In Section 2, we give the problem statement and prove a well-posedness result for the weak problem. A conforming finite element scheme is introduced in Section 3, where stability and convergence results are also settled. In order to design an adaptive procedure, we propose in Section 4 a residual a posteriori error estimator and prove its reliability and efficiency. Finally, the method and the estimator are tested in Section 5.

2. The model problem

We consider the problem of determining the response to prescribed static forces of an elastic solid containing a barotropic and inviscid fluid at rest.

We denote by Ω_F and Ω_S the reference domains for the fluid and the solid, respectively. More precisely, let $\Omega_F \subset \mathbb{R}^N$, $N = 2$ or 3, be a bounded open set (for simplicity we will suppose Ω_F connected) with Lipschitz polyhedral boundary Γ_I. Let $\Gamma_I^1, \dots, \Gamma_I^M$ be the planar parts of Γ_I, so that $\Gamma_I = \bigcup_{j=1}^{M} \Gamma_I^j$. Let Ω_S be an 'annular' region surrounding Ω_F with Lipschitz polyhedral outer boundary $\Gamma = \Gamma_D \cup \Gamma_N$, where $|\Gamma_D| \neq 0$. Let $\boldsymbol{n}$ be the normal vector to Γ_I pointing towards the exterior of Ω_F and $\boldsymbol{\nu}$ the unit outward vector to Γ (see Fig. 1 for a sketch of the domains).

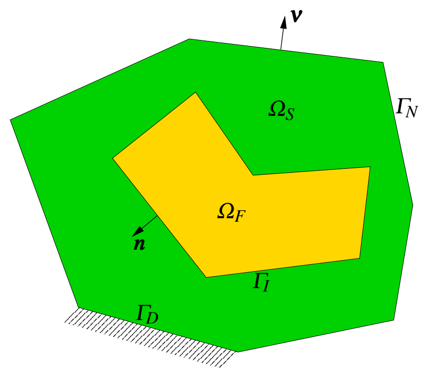

FIG. 1. Sketch of the domains.

Given volumetric force densities $\boldsymbol{f}_S \in L^2(\Omega_S)^N$ and $\boldsymbol{f}_F \in L^2(\Omega_F)^N$ ($\boldsymbol{f}_F$ being a gradient) and a surface force density $\boldsymbol{g} \in L^2(\Gamma_N)^N$, the classical elastoacoustics model for small-amplitude motions (see Morand & Ohayon (1995)) leads to the following static problem: find the solid displacement $\boldsymbol{u}$, the variation p of the fluid pressure and a scalar potential φ for the fluid displacement (i.e., the fluid displacement is given by $\nabla\varphi$), satisfying:

$$\nabla p = \boldsymbol{f}_F \qquad \text{in } \Omega_F, \tag{2.1}$$

$$\frac{1}{\rho_F c^2} p + \Delta\varphi = 0 \qquad \text{in } \Omega_F, \tag{2.2}$$

$$-\operatorname{div} \boldsymbol{\sigma}(\boldsymbol{u}) = \boldsymbol{f}_S \qquad \text{in } \Omega_S, \tag{2.3}$$

$$\frac{\partial\varphi}{\partial\boldsymbol{n}} = \boldsymbol{u}\cdot\boldsymbol{n} \qquad \text{on } \Gamma_I, \tag{2.4}$$

$$\boldsymbol{\sigma}(\boldsymbol{u})\boldsymbol{n} = -p\boldsymbol{n} \qquad \text{on } \Gamma_I, \tag{2.5}$$

$$\boldsymbol{\sigma}(\boldsymbol{u})\boldsymbol{\nu} = \boldsymbol{g} \qquad \text{on } \Gamma_N, \tag{2.6}$$

$$\boldsymbol{u} = \boldsymbol{0} \qquad \text{on } \Gamma_D. \tag{2.7}$$

In the equations above, ρ_F and c denote the density and the sound speed of the fluid, respectively. We assume that the stress and the strain tensors are related by the usual linear constitutive Hooke's law:

$$\boldsymbol{\sigma}(\boldsymbol{u}) := 2\mu\boldsymbol{\varepsilon}(\boldsymbol{u}) + \lambda \operatorname{tr}\boldsymbol{\varepsilon}(\boldsymbol{u})\boldsymbol{I}, \tag{2.8}$$

where $\lambda, \mu > 0$ are the Lamé coefficients, $\boldsymbol{\varepsilon}(\boldsymbol{u}) := \frac{1}{2}(\nabla\boldsymbol{u} + \nabla\boldsymbol{u}^t)$ is the linearized strain tensor and $\boldsymbol{I}$ is the $\mathbb{R}^{N\times N}$ identity matrix. An extension to more general materials is sketched in Appendix A.

The forthcoming analysis will be valid even for an incompressible fluid, in which case $c = \infty$. Because of this, all the physical parameters will be treated as fixed constants, except for the sound speed c, and in what follows we will obtain estimates with positive constants C, C', etc., not necessarily the same at each occurrence, but always independent of $c \geqslant c_0$ (c_0 being a fixed positive number).

REMARK 2.1 If the fluid is supposed to be incompressible, then equation (2.2) is replaced by $\Delta\varphi = 0$ in Ω_F.

Throughout this paper we will use standard notation for Sobolev spaces. Moreover, we denote $H^1_{\Gamma_D}(\Omega_S)$ the subspace of functions in $H^1(\Omega_S)$ with a vanishing trace on Γ_D. We will also use, as above, boldface symbols to denote vector and tensor fields.

In order to obtain a weak formulation of this problem, let us multiply (2.1) by $\nabla\psi$, with $\psi \in H^1(\Omega_F)/\mathbb{R}$, and integrate over Ω_F, which leads to

$$\int_{\Omega_F} \nabla p \cdot \nabla \psi = \int_{\Omega_F} \boldsymbol{f}_F \cdot \nabla \psi \qquad \forall \psi \in H^1(\Omega_F)/\mathbb{R}. \tag{2.9}$$

Next, (2.2) is tested against $q \in H^1(\Omega_F)$ to obtain

$$\int_{\Omega_F} \frac{1}{\rho_F c^2} pq - \int_{\Omega_F} \nabla\varphi \cdot \nabla q + \int_{\Gamma_I} \frac{\partial \varphi}{\partial \boldsymbol{n}} q = 0,$$

which, after application of the transmission condition (2.4) leads to

$$\int_{\Omega_F} \nabla\varphi \cdot \nabla q - \int_{\Gamma_I} q\boldsymbol{u}\cdot\boldsymbol{n} - \int_{\Omega_F} \frac{1}{\rho_F c^2} pq = 0 \qquad \forall q \in H^1(\Omega_F). \tag{2.10}$$

Finally, testing (2.3) against $\boldsymbol{v} \in H^1_{\Gamma_D}(\Omega_S)^N$ and applying the transmission conditions (2.4)–(2.5) we obtain (recall that $\boldsymbol{n}$ points towards Ω_S)

$$\int_{\Omega_S} \boldsymbol{\sigma}(\boldsymbol{u}) : \boldsymbol{\varepsilon}(\boldsymbol{v}) - \int_{\Gamma_I} p\boldsymbol{v}\cdot\boldsymbol{n} = \int_{\Omega_S} \boldsymbol{f}_S \cdot \boldsymbol{v} + \int_{\Gamma_N} \boldsymbol{g}\cdot\boldsymbol{v} \qquad \forall \boldsymbol{v} \in H^1_{\Gamma_D}(\Omega_S)^N. \tag{2.11}$$

Collecting (2.9), (2.10) and (2.11) we arrive at the following weak form of (2.1)–(2.7):
Find $(\boldsymbol{u}, \varphi, p) \in H^1_{\Gamma_D}(\Omega_S)^N \times H^1(\Omega_F)/\mathbb{R} \times H^1(\Omega_F)$ *such that*

$$\int_{\Omega_S} \boldsymbol{\sigma}(\boldsymbol{u}) : \boldsymbol{\varepsilon}(\boldsymbol{v}) + \int_{\Omega_F} \nabla\psi \cdot \nabla p - \int_{\Gamma_I} p\boldsymbol{v}\cdot\boldsymbol{n} = \int_{\Omega_S} \boldsymbol{f}_S \cdot \boldsymbol{v} + \int_{\Gamma_N} \boldsymbol{g}\cdot\boldsymbol{v} + \int_{\Omega_F} \boldsymbol{f}_F \cdot \nabla\psi, \tag{2.12}$$

$$\int_{\Omega_F} \nabla\varphi \cdot \nabla q - \int_{\Gamma_I} q\boldsymbol{u}\cdot\boldsymbol{n} - \int_{\Omega_F} \frac{1}{\rho_F c^2} pq = 0, \tag{2.13}$$

for all $(\boldsymbol{v}, \psi, q) \in H^1_{\Gamma_D}(\Omega_S)^N \times H^1(\Omega_F)/\mathbb{R} \times H^1(\Omega_F)$.

REMARK 2.2 If the fluid is supposed to be incompressible, we obtain a problem similar to (2.12)–(2.13), but without the term $\int_{\Omega_F} \frac{1}{\rho_F c^2} pq$, since the latter is already not present in (2.10).

REMARK 2.3 The variational problem (2.12)–(2.13) is well posed even for $\boldsymbol{f}_F$ not being a gradient. In such a case, a solution of this problem would only satisfy ∇p equal to the gradient part of a Helmholtz decomposition of $\boldsymbol{f}_F$.

Problem (2.12)–(2.13) may be written in an equivalent mildly coupled way. In fact, if we split $p = p_0 + c_p$, with $p_0 \in \widetilde{H}^1(\Omega_F) := \left\{ q \in H^1(\Omega_F) : \int_{\Omega_F} q = 0 \right\}$ and $c_p \in \mathbb{R}$, then, from (2.9) we see that p_0 satisfies

$$\int_{\Omega_F} \nabla p_0 \cdot \nabla \psi = \int_{\Omega_F} \boldsymbol{f}_F \cdot \nabla\psi \qquad \forall \psi \in \widetilde{H}^1(\Omega_F), \tag{2.14}$$

and this equation may be solved independently. Once p_0 is computed, (2.11) may be rewritten as follows:

$$\int_{\Omega_S} \boldsymbol{\sigma}(\boldsymbol{u}) : \boldsymbol{\varepsilon}(\boldsymbol{v}) - \int_{\Gamma_I} c_p \boldsymbol{v}\cdot\boldsymbol{n} = \int_{\Omega_S} \boldsymbol{f}_S \cdot \boldsymbol{v} + \int_{\Gamma_N} \boldsymbol{g}\cdot\boldsymbol{v} + \int_{\Gamma_I} p_0 \boldsymbol{v}\cdot\boldsymbol{n} \qquad \forall \boldsymbol{v} \in H^1_{\Gamma_D}(\Omega_S)^N.$$

This equation is undetermined. To be able to solve it, we need another equation which allows us to find the constant c_p. With this aim, we test the equation (2.10) with $q = 1$ to obtain

$$-\int_{\Gamma_I} \boldsymbol{u}\cdot\boldsymbol{n} - \frac{|\Omega_F|}{\rho_f c^2} c_p = 0.$$

Hence, we are lead to the following mixed problem for $(\boldsymbol{u}, c_p)$:

$$\begin{aligned} &\int_{\Omega_S} \boldsymbol{\sigma}(\boldsymbol{u}) : \boldsymbol{\varepsilon}(\boldsymbol{v}) - \int_{\Gamma_I} c_p \boldsymbol{v}\cdot\boldsymbol{n} = \int_{\Omega_S} \boldsymbol{f}_S \cdot \boldsymbol{v} + \int_{\Gamma_N} \boldsymbol{g}\cdot\boldsymbol{v} + \int_{\Gamma_I} p_0 \boldsymbol{v}\cdot\boldsymbol{n} \qquad && \forall \boldsymbol{v} \in H^1_{\Gamma_D}(\Omega_S)^N, \\ &-\int_{\Gamma_I} d_p \boldsymbol{u}\cdot\boldsymbol{n} - \frac{|\Omega_F|}{\rho_f c^2} d_p c_p = 0 && \forall d_p \in \mathbb{R}. \end{aligned} \tag{2.15}$$

It is immediate to show that this mixed problem is well posed. Finally, once $\boldsymbol{u}$ and c_p are computed, we can obtain φ as the solution of (2.10) for test functions belonging to $H^1(\Omega_F)/\mathbb{R}$, namely,

$$\int_{\Omega_F} \nabla\varphi\cdot\nabla q = \int_{\Gamma_I} q\boldsymbol{u}\cdot\boldsymbol{n} + \int_{\Omega_F} \frac{1}{\rho_F c^2}\,(p_0 + c_p)\,q \qquad \forall q \in H^1(\Omega_F)/\mathbb{R}. \tag{2.16}$$

This is a well posed Neumann problem, by virtue of the second equation of (2.15).

In principle, any of the formulations, (2.12)–(2.13) or (2.14)–(2.16) can be discretized by standard finite elements. It is simple to show that the resulting discrete problems are also equivalent, provided the same elements are used in both formulations for each variable. The mildly coupled formulation (2.14)–(2.16) leads, of course, to a less expensive implementation. In fact, this is the formulation we have used for our numerical experiments. However, for the error analysis of the finite element method, we will use the coupled formulation (2.12)–(2.13), which avoids dealing with non-conforming terms in the right-hand sides of (2.15) and (2.16). Such approach makes it easier to obtain higher order a priori error estimates in L^2 norm (cf. Subsection 3.1) and, particularly, it allows us to derive a posteriori error estimates (cf. Section 4).

To analyze the coupled formulation, consider the Hilbert spaces $\mathscr{X} := H^1_{\Gamma_D}(\Omega_S)^N \times H^1(\Omega_F)/\mathbb{R}$ and $\mathscr{M} := H^1(\Omega_F)$, equipped with their natural norms, the continuous bilinear forms $a : \mathscr{X}\times\mathscr{X} \to \mathbb{R}$, $b : \mathscr{X}\times\mathscr{M} \to \mathbb{R}$ and $d : \mathscr{M}\times\mathscr{M} \to \mathbb{R}$, respectively defined by

$$\begin{aligned} a((\boldsymbol{u},\varphi),(\boldsymbol{v},\psi)) &:= \int_{\Omega_S} \boldsymbol{\sigma}(\boldsymbol{u}) : \boldsymbol{\varepsilon}(\boldsymbol{v}), && (\boldsymbol{u},\varphi),(\boldsymbol{v},\psi) \in \mathscr{X}, \\ b((\boldsymbol{v},\psi),q) &:= \int_{\Omega_F} \nabla\psi\cdot\nabla q - \int_{\Gamma_I} q\boldsymbol{v}\cdot\boldsymbol{n}, && (\boldsymbol{v},\psi) \in \mathscr{X},\ q \in \mathscr{M}, \\ d(p,q) &:= \int_{\Omega_F} \frac{1}{\rho_F c^2}\, pq, && p,q \in \mathscr{M}, \end{aligned}$$

and the linear functional $\boldsymbol{F} \in \mathscr{X}'$ given by

$$\boldsymbol{F}(\boldsymbol{v},\psi) := \int_{\Omega_S} \boldsymbol{f}_S\cdot\boldsymbol{v} + \int_{\Gamma_N} \boldsymbol{g}\cdot\boldsymbol{v} + \int_{\Omega_F} \boldsymbol{f}_F\cdot\nabla\psi, \qquad (\boldsymbol{v},\psi) \in \mathscr{X}.$$

Then, the weak problem (2.12)–(2.13) reads as follows:

Find $((\boldsymbol{u},\varphi),p)\in\mathscr{X}\times\mathscr{M}$ *such that*

$$a((\boldsymbol{u},\varphi),(\boldsymbol{v},\psi))+b((\boldsymbol{v},\psi),p)=\boldsymbol{F}(\boldsymbol{v},\psi) \qquad \forall(\boldsymbol{v},\psi)\in\mathscr{X}, \tag{2.17}$$

$$b((\boldsymbol{u},\varphi),q)-d(p,q)=0 \qquad \forall q\in\mathscr{M}. \tag{2.18}$$

To analyze this problem we define the kernel

$$\begin{aligned}\mathscr{Z}&:=\{(\boldsymbol{v},\psi)\in\mathscr{X}:\ b((\boldsymbol{v},\psi),q)=0\quad\forall q\in\mathscr{M}\}\\&=\left\{(\boldsymbol{v},\psi)\in\mathscr{X}:\ \int_{\Omega_F}\nabla\psi\cdot\nabla q-\int_{\Gamma_I}q\boldsymbol{v}\cdot\boldsymbol{n}=0\quad\forall q\in\mathscr{M}\right\}.\end{aligned} \tag{2.19}$$

LEMMA 2.1 The bilinear form a is $\mathscr{X}$-elliptic in $\mathscr{Z}$, namely, there exists a constant $\alpha>0$ such that

$$a((\boldsymbol{v},\psi),(\boldsymbol{v},\psi))\geqslant\alpha\,\|(\boldsymbol{v},\psi)\|_{\mathscr{X}}^2\qquad\forall(\boldsymbol{v},\psi)\in\mathscr{Z}.$$

Proof. Let $(\boldsymbol{v},\psi)\in\mathscr{Z}$. From the definition of a and Korn's inequality it follows that, for all $(\boldsymbol{v},\psi)\in\mathscr{Z}$,

$$a((\boldsymbol{v},\psi),(\boldsymbol{v},\psi))=\int_{\Omega_S}\boldsymbol{\sigma}(\boldsymbol{v}):\boldsymbol{\varepsilon}(\boldsymbol{v})\geqslant C\,\|\boldsymbol{v}\|_{1,\Omega_S}^2. \tag{2.20}$$

Next, from the definition of $\mathscr{Z}$ we observe that, choosing $q=\psi_0$ in (2.19), ψ_0 being the element of the equivalence class of ψ satisfying $\int_{\Omega_F}\psi_0=0$, applying the trace theorem in Ω_S and Ω_F, and the Poincaré-Friedrichs inequality, we obtain

$$|\psi|_{1,\Omega_F}^2=\int_{\Gamma_I}\psi_0\boldsymbol{v}\cdot\boldsymbol{n}\leqslant\|\psi_0\|_{0,\Gamma_I}\,\|\boldsymbol{v}\cdot\boldsymbol{n}\|_{0,\Gamma_I}\leqslant C\,|\psi_0|_{1,\Omega_F}\,\|\boldsymbol{v}\|_{1,\Omega_S},$$

which together with (2.20) yield the result. □

The inf-sup condition for b is stated in the next result.

LEMMA 2.2 There exists a constant $\beta>0$ such that

$$\sup_{(\boldsymbol{v},\psi)\in\mathscr{X}\setminus\{\boldsymbol{0}\}}\frac{b((\boldsymbol{v},\psi),q)}{\|(\boldsymbol{v},\psi)\|_{\mathscr{X}}}\geqslant\beta\,\|q\|_{\mathscr{M}}\qquad\forall q\in\mathscr{M}.$$

Proof. Let $q\in\mathscr{M}$. First, we easily see that

$$\sup_{(\boldsymbol{v},\psi)\in\mathscr{X}\setminus\{\boldsymbol{0}\}}\frac{b((\boldsymbol{v},\psi),q)}{\|(\boldsymbol{v},\psi)\|_{\mathscr{X}}}\geqslant\sup_{\psi\in H^1(\Omega_F)/\mathbb{R}\setminus\{\boldsymbol{0}\}}\frac{\int_{\Omega_F}\nabla\psi\cdot\nabla q}{|\psi|_{1,\Omega_F}}=|q|_{1,\Omega_F}. \tag{2.21}$$

On the other hand, let $\hat{\boldsymbol{z}}$ be the vector field defined by $\hat{\boldsymbol{z}}(\boldsymbol{x}):=x_1\boldsymbol{e}_1$, where $\boldsymbol{e}_1:=(1,0)$ in $\mathbb{R}^2$ and $\boldsymbol{e}_1:=(1,0,0)$ in $\mathbb{R}^3$. Also, let χ be a cutoff function belonging to $\mathscr{C}_0^\infty(\overline{\Omega}_F\cup\Omega_S)$ such that $\chi=1$ in an open set containing $\overline{\Omega}_F$. Then, $\boldsymbol{z}:=\chi\hat{\boldsymbol{z}}|_{\Omega_S}\in H^1_{\Gamma_D}(\Omega_S)^N$ and

$$\int_{\Gamma_I}\boldsymbol{z}\cdot\boldsymbol{n}=\int_{\Gamma_I}\hat{\boldsymbol{z}}\cdot\boldsymbol{n}=\int_{\Omega_F}\operatorname{div}\hat{\boldsymbol{z}}=|\Omega_F|>0.$$

Hence, the linear form defined by $f(q) := \int_{\Gamma_I} q\boldsymbol{z}\cdot\boldsymbol{n}$ belongs to $H^1(\Omega_F)'$ (thanks to the trace theorem) and is such that $f(1) \neq 0$. Hence, applying the generalized Poincaré's inequality (cf. (Ern & Guermond, 2004, Lemma B63)), there exists a constant $C > 0$, depending only on Ω_F and $\boldsymbol{z}$ such that, for all $q \in H^1(\Omega_F)$,

$$C\|q\|_{1,\Omega_F} \leqslant |q|_{1,\Omega_F} + |f(q)| \leqslant |q|_{1,\Omega_F} + \|\boldsymbol{z}\|_{1,\Omega_S} \sup_{\boldsymbol{v}\in H^1_{\Gamma_D}(\Omega_S)^N\setminus\{\boldsymbol{0}\}} \frac{\int_{\Gamma_I} q\boldsymbol{v}\cdot\boldsymbol{n}}{\|\boldsymbol{v}\|_{1,\Omega_S}}$$
$$\leqslant |q|_{1,\Omega_F} + \|\boldsymbol{z}\|_{1,\Omega_S} \sup_{(\boldsymbol{v},\psi)\in\mathscr{X}\setminus\{\boldsymbol{0}\}} \frac{b((\boldsymbol{v},\psi),q)}{\|(\boldsymbol{v},\psi)\|_{\mathscr{X}}},$$

which together with (2.21) yield the inf-sup condition with a constant $\beta := C/(1+\|\boldsymbol{z}\|_{1,\Omega_S})$. □

THEOREM 2.1 There exists a unique $((\boldsymbol{u},\varphi),p) \in \mathscr{X}\times\mathscr{M}$ solution of problem (2.17)–(2.18) and there exists a constant $C > 0$, independent of c, such that

$$\|\boldsymbol{u}\|_{1,\Omega_S} + |\varphi|_{1,\Omega_F} + \|p\|_{1,\Omega_F} \leqslant C\left(\|\boldsymbol{f}_S\|_{0,\Omega_S} + \|\boldsymbol{f}_F\|_{0,\Omega_F} + \|\boldsymbol{g}\|_{0,\Gamma_N}\right).$$

Proof. By virtue of Lemmas 2.1 and 2.2, it is enough to take into account that the bilinear form d is positive definite in $\mathscr{M}$ and satisfies the assumptions of Case 3 from (Brezzi & Fortin, 1991, p. 47), to apply Theorem 1.2 from the same reference. □

REMARK 2.4 The existence and uniqueness result given above is also valid if the fluid is incompressible, i.e., if $d(p,q) \equiv 0$, in which case it is a direct consequence of the classical theory for mixed problems (cf. Brezzi & Fortin (1991)).

REMARK 2.5 Let us define the bilinear form $\mathscr{B} : (\mathscr{X}\times\mathscr{M})\times(\mathscr{X}\times\mathscr{M}) \longrightarrow \mathbb{R}$ given by

$$\mathscr{B}(((\boldsymbol{u},\varphi),p),((\boldsymbol{v},\psi),q)) := a((\boldsymbol{u},\varphi),(\boldsymbol{v},\psi)) + b((\boldsymbol{v},\psi),p) + b((\boldsymbol{u},\varphi),p) - d(p,q).$$

Then (cf. (Braess & Blömer, 1990, Lemma B.1)), there exists a constant $C_{\mathscr{B}}$, independent of c, such that, for all $((\boldsymbol{v},\psi),q) \in \mathscr{X}\times\mathscr{M}$,

$$\|((\boldsymbol{v},\psi),q)\|_{\mathscr{X}\times\mathscr{M}} \leqslant C_{\mathscr{B}} \sup_{((\boldsymbol{w},\xi),r)\in\mathscr{X}\times\mathscr{M}\setminus\{\boldsymbol{0}\}} \frac{\mathscr{B}(((\boldsymbol{v},\psi),q),((\boldsymbol{w},\xi),r))}{\|((\boldsymbol{w},\xi),r)\|_{\mathscr{X}\times\mathscr{M}}}. \tag{2.22}$$

3. The finite element scheme

Let $\{\mathscr{T}_h^F\}_{h>0}$ and $\{\mathscr{T}_h^S\}_{h>0}$ be regular families of triangulations (tetrahedral meshes, if $N = 3$) of $\overline{\Omega}_F$ and $\overline{\Omega}_S$, respectively, which may be chosen independently. In particular, they do not need to match on the common boundary Γ_I. Given a couple of meshes, $\mathscr{T}_h^F$ and $\mathscr{T}_h^S$, the mesh-size is defined by $h := \max_{K\in\mathscr{T}_h^F\cup\mathscr{T}_h^S} h_K$, with h_K being the diameter of K. From now on, the generic constants C, C', etc, will not only be independent of $c \geqslant c_0$, but also independent of the mesh-size h.

Let $k,l,m \geqslant 1$ and let us define the following finite element spaces:

$$\mathscr{H}_h := \left\{\boldsymbol{v}_h \in \mathscr{C}^0(\overline{\Omega}_S)^N : \boldsymbol{v}_h|_K \in \mathbb{P}_k(K)^N \quad \forall K \in \mathscr{T}_h^S\right\} \cap H^1_{\Gamma_D}(\Omega_S)^N,$$
$$\mathscr{V}_h := \left\{\psi_h \in \mathscr{C}^0(\overline{\Omega}_F) : \psi_h|_K \in \mathbb{P}_l(K) \quad \forall K \in \mathscr{T}_h^F\right\},$$
$$\mathscr{M}_h := \left\{q_h \in \mathscr{C}^0(\overline{\Omega}_F) : q_h|_K \in \mathbb{P}_m(K) \quad \forall K \in \mathscr{T}_h^F\right\}.$$

For reasons that will become clear in what follows, we take $l \geqslant m$. Defining $\mathscr{X}_h := \mathscr{H}_h \times \mathscr{V}_h/\mathbb{R}$, the finite element scheme associated to (2.17)–(2.18) reads as follows:

Find $((\boldsymbol{u}_h, \varphi_h), p_h) \in \mathscr{X}_h \times \mathscr{M}_h$ *such that*

$$a((\boldsymbol{u}_h, \varphi_h), (\boldsymbol{v}_h, \psi_h)) + b((\boldsymbol{v}_h, \psi_h), p_h) = \boldsymbol{F}(\boldsymbol{v}_h, \psi_h) \qquad \forall (\boldsymbol{v}_h, \psi_h) \in \mathscr{X}_h, \tag{3.1}$$

$$b((\boldsymbol{u}_h, \varphi_h), q_h) - d(p_h, q_h) = 0 \qquad \forall q_h \in \mathscr{M}_h. \tag{3.2}$$

We obtain the following result by repeating the arguments used to prove Lemma 2.1.

LEMMA 3.1 Let

$$\mathscr{Z}_h := \{(\boldsymbol{v}_h, \psi_h) \in \mathscr{X}_h : \ b((\boldsymbol{v}_h, \psi_h), q_h) = 0 \quad \forall q_h \in \mathscr{M}_h\}.$$

Then, for the same constant $\alpha > 0$ from Lemma 2.1 (independent of h), there holds

$$a((\boldsymbol{v}_h, \psi_h), (\boldsymbol{v}_h, \psi_h)) \geqslant \alpha \, \|(\boldsymbol{v}_h, \psi_h)\|_{\mathscr{X}}^2 \qquad \forall (\boldsymbol{v}_h, \psi_h) \in \mathscr{Z}_h.$$

The discrete inf-sup condition for the bilinear form b is proved next.

LEMMA 3.2 There exists $\beta_* > 0$, independent of h, such that

$$\sup_{(\boldsymbol{v}_h, \psi_h) \in \mathscr{X}_h \setminus \{\boldsymbol{0}\}} \frac{b((\boldsymbol{v}_h, \psi_h), q_h)}{\|(\boldsymbol{v}_h, \psi_h)\|_{\mathscr{X}}} \geqslant \beta_* \, \|q_h\|_{\mathscr{M}} \qquad \forall q_h \in \mathscr{M}_h.$$

Proof. Let $q_h \in \mathscr{M}_h$. Since $l \geqslant m$, we proceed as in the proof of Lemma 2.2 to obtain

$$\sup_{(\boldsymbol{v}_h, \psi_h) \in \mathscr{X}_h \setminus \{\boldsymbol{0}\}} \frac{b((\boldsymbol{v}_h, \psi_h), q_h)}{\|(\boldsymbol{v}_h, \psi_h)\|_{\mathscr{X}}} \geqslant |q_h|_{1,\Omega_F}.$$

On the other hand, considering $\hat{\boldsymbol{z}}$ and $\boldsymbol{z}$ as in the proof of Lemma 2.2, we have

$$C \, \|q_h\|_{1,\Omega_F} \leqslant |q_h|_{1,\Omega_F} + \left| \int_{\Gamma_I} q_h \boldsymbol{z} \cdot \boldsymbol{n} \right|.$$

Next, let $\boldsymbol{z}_h \in \mathscr{H}_h$ be the Scott-Zhang interpolant of $\boldsymbol{z}$ (see Scott & Zhang (1990); Brenner & Scott (1994)), where the interpolation is taken component-wise. Then, since $\boldsymbol{z}|_{\Gamma_I} = \hat{\boldsymbol{z}}|_{\Gamma_I}$ is an affine function, we have that $\boldsymbol{z}_h|_{\Gamma_I} = \boldsymbol{z}|_{\Gamma_I}$ and, moreover, from the approximation properties of this interpolant (cf. Brenner & Scott (1994); Ern & Guermond (2004)) we obtain

$$\|\boldsymbol{z}_h\|_{1,\Omega_S} \leqslant C' \, \|\boldsymbol{z}\|_{1,\Omega_S},$$

where $C' > 0$ does not depend on h. We then arrive at

$$\int_{\Gamma_I} q_h \boldsymbol{z} \cdot \boldsymbol{n} = \int_{\Gamma_I} q_h \boldsymbol{z}_h \cdot \boldsymbol{n} = \|\boldsymbol{z}_h\|_{1,\Omega_S} \frac{\int_{\Gamma_I} q_h \boldsymbol{z}_h \cdot \boldsymbol{n}}{\|\boldsymbol{z}_h\|_{1,\Omega_S}} \leqslant C' \, \|\boldsymbol{z}\|_{1,\Omega_S} \sup_{(\boldsymbol{v}_h, \psi_h) \in \mathscr{X}_h \setminus \{\boldsymbol{0}\}} \frac{b((\boldsymbol{v}_h, \psi_h), q_h)}{\|(\boldsymbol{v}_h, \psi_h)\|_{\mathscr{X}}},$$

and the result follows with $\beta_* := C/(1 + C' \, \|\boldsymbol{z}\|_{1,\Omega_S})$. □

REMARK 3.1 We stress the fact that the constant β_* depends only on Ω_F, Ω_S and $\boldsymbol{z}$, but, thanks to the choice made for the latter, it does not depend on the mesh-size h.

As a consequence of the above lemmas, we obtain the main result of this section.

THEOREM 3.1 There exists a unique solution $((\boldsymbol{u}_h,\varphi_h),p_h)\in\mathscr{X}_h\times\mathscr{M}_h$ of problem (3.1)–(3.2) and there exists a positive constant $C>0$, independent of h and c, such that

$$\begin{aligned}\|\boldsymbol{u}-\boldsymbol{u}_h\|_{1,\Omega_S}+|\varphi-\varphi_h|_{1,\Omega_F}+\|p-p_h\|_{1,\Omega_F}&\\ \leqslant C\left(\inf_{\boldsymbol{v}_h\in\mathscr{H}_h}\|\boldsymbol{u}-\boldsymbol{v}_h\|_{1,\Omega_S}+\inf_{\psi_h\in\mathscr{V}_h}|\varphi-\psi_h|_{1,\Omega_F}+\inf_{q_h\in\mathscr{M}_h}\|p-q_h\|_{1,\Omega_F}\right),&\end{aligned}$$

where $((\boldsymbol{u},\varphi),p)\in\mathscr{X}\times\mathscr{M}$ is the unique solution of problem (2.17)–(2.18).

Proof. It is enough to apply Proposition 2.11, from (Brezzi & Fortin, 1991, Chap. II). □

REMARK 3.2 The previous result provides an error estimate which is robust with respect to large values of the bulk modulus $\rho_F c^2$ and covers the incompressible case in which $d(p,q)=0$.

REMARK 3.3 Although in practice the most usual is to take equal order elements for all variables, the choice of interpolation spaces is arbitrary. In principle, the only constraint is the one used in Lemma 3.2: $l\geqslant m$. However, even this can be avoided. In fact, Theorem 3.1 can be alternatively proved without assuming $l\geqslant m$ by analyzing the discretization of the mildly coupled problem (2.14)–(2.16). Finally notice that, since the meshes for the fluid and the solid do not need to satisfy any compatibility condition on the interface, completely independent refinement procedures may be considered in each domain.

3.1 *An error estimate in the L^2 norms*

The purpose of this section is to obtain higher order error estimates in the L^2 norm for all the variables. To do this, let $((\boldsymbol{u},\varphi),p)$ and $((\boldsymbol{u}_h,\varphi_h),p_h)$ be the solutions of (2.17)–(2.18) and (3.1)–(3.2), respectively, where we have fixed representatives of $\varphi\in H^1(\Omega_F)/\mathbb{R}$ and $\varphi_h\in\mathscr{V}_h/\mathbb{R}$, still denoted φ and φ_h, satisfying $\int_{\Omega_F}\varphi=\int_{\Omega_F}\varphi_h=0$. Next, let $((\boldsymbol{w},\xi),r)\in\mathscr{X}\times\mathscr{M}$ be the solution of the dual problem:

$$a((\boldsymbol{w},\xi),(\boldsymbol{v},\psi))+b((\boldsymbol{v},\psi),r)=\int_{\Omega_S}(\boldsymbol{u}-\boldsymbol{u}_h)\cdot\boldsymbol{v}+\int_{\Omega_F}(\varphi-\varphi_h)\,\psi\qquad\forall(\boldsymbol{v},\psi)\in\mathscr{X},\tag{3.3}$$

$$b((\boldsymbol{w},\xi),q)-d(r,q)=\int_{\Omega_F}(p-p_h)\,q\qquad\forall q\in\mathscr{M}.\tag{3.4}$$

The same arguments used in the proof of Theorem 2.1 allow us to show that (3.3)–(3.4) admits a unique solution $((\boldsymbol{w},\xi),r)$ satisfying

$$\|\boldsymbol{w}\|_{1,\Omega_S}+|\xi|_{1,\Omega_F}+\|r\|_{1,\Omega_F}\leqslant C\left(\|\boldsymbol{u}-\boldsymbol{u}_h\|_{0,\Omega_F}+\|\varphi-\varphi_h\|_{0,\Omega_F}+\|p-p_h\|_{0,\Omega_F}\right),\tag{3.5}$$

where $C>0$ is again independent of c.

Now, considering $\boldsymbol{v}=\mathbf{0}$ in (3.3), we obtain that $r\in H^1(\Omega_F)$ is a solution of the compatible Neumann problem

$$\begin{aligned}-\Delta r&=\varphi-\varphi_h&&\text{in }\Omega_F,\\ \frac{\partial r}{\partial\boldsymbol{n}}&=0&&\text{on }\Gamma_I.\end{aligned}$$

Hence (cf. Grisvard (1985)), there exists $s > \frac{1}{2}$ such that $r \in H^{1+s}(\Omega_F)$ and $\|\nabla r\|_{s,\Omega_F} \leqslant C\,\|\varphi - \varphi_h\|_{0,\Omega_F}$, which together with (3.5) show that

$$\|r\|_{1+s,\Omega_F} \leqslant C\left(\|\boldsymbol{u}-\boldsymbol{u}_h\|_{0,\Omega_F} + \|\varphi-\varphi_h\|_{0,\Omega_F} + \|p-p_h\|_{0,\Omega_F}\right). \tag{3.6}$$

On the other hand, taking $\psi = 0$ in (3.3), we have that $\boldsymbol{w}$ is the weak solution of

$$\begin{aligned} -\operatorname{div}\boldsymbol{\sigma}(\boldsymbol{w}) &= \boldsymbol{u}-\boldsymbol{u}_h && \text{in } \Omega_S,\\ \boldsymbol{\sigma}(\boldsymbol{w})\boldsymbol{n} &= r\boldsymbol{n} && \text{on } \Gamma_I,\\ \boldsymbol{\sigma}(\boldsymbol{w})\boldsymbol{\nu} &= \boldsymbol{0} && \text{on } \Gamma_N,\\ \boldsymbol{w} &= \boldsymbol{0} && \text{on } \Gamma_D. \end{aligned}$$

Hence (cf. Grisvard (1985)), since $r\boldsymbol{n} \in H^{\frac{1}{2}}(\Gamma_I^j)^N$, $j = 1,\dots,M$, there exists $t > 0$ such that $\boldsymbol{w} \in H^{1+t}(\Omega_S)^N$ and

$$\begin{aligned} \|\boldsymbol{w}\|_{1+t,\Omega_S} &\leqslant C\left(\|\boldsymbol{u}-\boldsymbol{u}_h\|_{0,\Omega_S} + \sum_{j=1}^{M}\|r\boldsymbol{n}\|_{1/2,\Gamma_I^j}\right) \leqslant C\left(\|\boldsymbol{u}-\boldsymbol{u}_h\|_{0,\Omega_S} + \|r\|_{1,\Omega_F}\right)\\ &\leqslant C\left(\|\boldsymbol{u}-\boldsymbol{u}_h\|_{0,\Omega_S} + \|\varphi-\varphi_h\|_{0,\Omega_F} + \|p-p_h\|_{0,\Omega_F}\right), \end{aligned} \tag{3.7}$$

the last inequality because of (3.5).

Finally, (3.4) implies that ξ satisfies

$$\begin{aligned} -\Delta\xi &= \frac{1}{\rho_F c^2} r + (p-p_h) && \text{in } \Omega_F,\\ \frac{\partial\xi}{\partial\boldsymbol{n}} &= \boldsymbol{w}\cdot\boldsymbol{n} && \text{on } \Gamma_I, \end{aligned}$$

and, since $\boldsymbol{w}\cdot\boldsymbol{n} \in H^{\frac{1}{2}}(\Gamma_I^j)$, $j = 1,\dots,M$, $\xi \in H^{1+s}(\Omega_F)/\mathbb{R}$ (cf. Grisvard (1985)) and

$$\begin{aligned} \|\nabla\xi\|_{s,\Omega_F} &\leqslant C\left(\left\|\frac{1}{\rho_F c^2} r + (p-p_h)\right\|_{0,\Omega_F} + \sum_{j=1}^{N}\|\boldsymbol{w}\cdot\boldsymbol{n}\|_{1/2,\Gamma_I^j}\right)\\ &\leqslant C\left(\|\boldsymbol{u}-\boldsymbol{u}_h\|_{0,\Omega_S} + \|\varphi-\varphi_h\|_{0,\Omega_F} + \|p-p_h\|_{0,\Omega_F}\right), \end{aligned} \tag{3.8}$$

the latter again from (3.5). Notice that C is independent of c (of course, for $c \geqslant c_0$). From these considerations we may state the following result.

THEOREM 3.2 There exist constants $C > 0$, $s > \frac{1}{2}$ and $t > 0$, all independent of h and c, such that

$$\begin{aligned} &\|\boldsymbol{u}-\boldsymbol{u}_h\|_{0,\Omega_S} + \|\varphi-\varphi_h\|_{0,\Omega_F} + \|p-p_h\|_{0,\Omega_F}\\ &\qquad \leqslant Ch^{\min\{s,t\}}\left(\|\boldsymbol{u}-\boldsymbol{u}_h\|_{1,\Omega_S} + |\varphi-\varphi_h|_{1,\Omega_F} + \|p-p_h\|_{1,\Omega_F}\right). \end{aligned}$$

Proof. Let $((\boldsymbol{w},\xi),r) \in \mathscr{X}\times\mathscr{M}$ be the solution of the dual problem (3.3)–(3.4) and $\boldsymbol{w}_h$, ξ_h and r_h the respective Scott-Zhang interpolants (cf. Scott & Zhang (1990)). Then, considering $((\boldsymbol{v},\psi),q) = ((\boldsymbol{u}-\boldsymbol{u}_h,\varphi-\varphi_h),p-p_h)$ in (3.3)–(3.4), using the Galerkin orthogonality, the continuity of a, b and d, and the approximation properties of the Scott-Zhang interpolation (cf. Scott & Zhang (1990); Ern & Guermond (2004)), we arrive at

$$\begin{aligned}
&\|\boldsymbol{u}-\boldsymbol{u}_h\|_{0,\Omega_S}^2+\|\varphi-\varphi_h\|_{0,\Omega_F}^2+\|p-p_h\|_{0,\Omega_F}^2\\
&\quad=\mathscr{B}\left(((\boldsymbol{w},\xi),r),((\boldsymbol{u}-\boldsymbol{u}_h,\varphi-\varphi_h),p-p_h)\right)\\
&\quad=\mathscr{B}\left(((\boldsymbol{u}-\boldsymbol{u}_h,\varphi-\varphi_h),p-p_h),((\boldsymbol{w}-\boldsymbol{w}_h,\xi-\xi_h),r-r_h)\right)\\
&\quad\leqslant C\Bigg[|\boldsymbol{u}-\boldsymbol{u}_h|_{1,\Omega_S}|\boldsymbol{w}-\boldsymbol{w}_h|_{1,\Omega_S}+\Big(\|\boldsymbol{w}-\boldsymbol{w}_h\|_{1,\Omega_S}+|\xi-\xi_h|_{1,\Omega_F}\Big)\|p-p_h\|_{1,\Omega_F}\\
&\qquad\quad+\Big(\|\boldsymbol{u}-\boldsymbol{u}_h\|_{1,\Omega_S}+|\varphi-\varphi_h|_{1,\Omega_F}\Big)\|r-r_h\|_{1,\Omega_F}+\frac{1}{\rho_F c^2}\|r-r_h\|_{0,\Omega_F}\|p-p_h\|_{0,\Omega_F}\Bigg]\\
&\quad\leqslant Ch^{\min\{s,t\}}\Big(\|\boldsymbol{u}-\boldsymbol{u}_h\|_{1,\Omega_S}^2+|\varphi-\varphi_h|_{1,\Omega_F}^2+\|p-p_h\|_{1,\Omega_F}^2\Big)^{\frac{1}{2}}\Big(|\boldsymbol{w}|_{1+t,\Omega_S}^2+|\xi|_{1+s,\Omega_F}^2+|r|_{1+s,\Omega_F}^2\Big)^{\frac{1}{2}},
\end{aligned}$$

and the result follows by using (3.6), (3.7) and (3.8). □

4. A residual a posteriori error estimation

4.1 *Preliminaries*

In this section, for simplicity, we will suppose that the prescribed force densities, $\boldsymbol{f}_S$, $\boldsymbol{f}_F$ and $\boldsymbol{g}$, are all piecewise polynomial functions. Also for simplicity, we will mainly use two-dimensional notation. However, the definition of the estimator and the properties proved in Theorem 4.1 below hold in the three-dimensional case, as well.

We restrict the analysis of this section to meshes in Ω_F and Ω_S matching on the common boundary Γ_I. The definition of the estimator introduced in the following subsection holds for non-matching grids too. However, some of the preliminary results which will be used in the sequel are not valid for general non-matching grids, for instance, the first inequality in (4.2) below.

We use the following notation:

- $\mathscr{E}_h^S$ and $\mathscr{E}_h^F$: sets of edges (faces, if $N=3$) of $\mathscr{T}_h^S$ and $\mathscr{T}_h^F$, respectively,
- $\widetilde{\mathscr{E}}_h^S$ and $\widetilde{\mathscr{E}}_h^F$: sets of inner edges (faces) of $\mathscr{T}_h^S$ and $\mathscr{T}_h^F$, respectively,
- $\mathscr{E}_h^N$ and $\mathscr{E}_h^D$: sets of edges (faces) of $\mathscr{T}_h^S$ lying on Γ_D and Γ_N, respectively,
- $\mathscr{E}_h^I$: set of common edges (faces) of $\mathscr{T}_h^S$ and $\mathscr{T}_h^F$ lying on Γ_I,
- $\mathscr{E}_K$: set of edges (faces) of $K\in\mathscr{T}_h^S\cup\mathscr{T}_h^F$,
- $\omega_K^S:=\bigcup\left\{K'\in\mathscr{T}_h^S:\ \mathscr{E}_{K'}\cap\mathscr{E}_K\neq\emptyset\right\}$, for $K\in\mathscr{T}_h^S$,
- $\omega_\ell^S:=\bigcup\left\{K\in\mathscr{T}_h^S:\ \ell\in\mathscr{E}_K\right\}$, for $\ell\in\mathscr{E}_h^S$.

We define in an analogous way the neighborhoods ω_K^F and ω_ℓ^F for $K\in\mathscr{T}_h^F$ and $\ell\in\mathscr{E}_h^F$. Moreover, we will write ω_K and ω_ℓ when it is not necessary to distinguish the medium. Furthermore, for $\ell\in\mathscr{E}_h^I$, we denote $K_\ell^F\in\mathscr{T}_h^F$ and $K_\ell^S\in\mathscr{T}_h^S$ the elements in each medium such that $\ell=K_\ell^F\cap K_\ell^S$.

For $K\in\mathscr{T}_h^S\cup\mathscr{T}_h^F$, let b_K be the classical bubble function in K:

$$b_K:=(N+1)^{N+1}\Pi_{j=0}^N\lambda_j^K,$$

where $\lambda_0^K,\dots,\lambda_N^K$ stand for the barycentric coordinates of K. For $\ell\in\mathscr{E}_h^S\cup\mathscr{E}_h^F$, let b_ℓ be the piecewise quadratic (cubic, if $N=3$) continuous function defined in ω_ℓ as follows:

$$b_\ell|_K := N^N \Pi_{j=1}^N \lambda_j^K, \qquad K\subset\omega_\ell,$$

with $\lambda_1^K,\dots,\lambda_N^K$ being the barycentric coordinates of K associated to the vertices of ℓ.

By using standard scaling arguments (cf. Verfürth (1996)) it can be proved that there exists a constant $C>0$ such that

$$C\,\|s\|_{0,K}^2 \leqslant \int_K b_K s^2 \leqslant \|s\|_{0,K}^2 \qquad \forall s\in\mathbb{P}_n(K), \tag{4.1}$$

$$C\,\|s\|_{0,\ell}^2 \leqslant \int_\ell b_\ell s^2 \leqslant \|s\|_{0,\ell}^2 \qquad \forall s\in\mathbb{P}_n(\ell). \tag{4.2}$$

The constant C depends on the degree n of the polynomial function and on the shape ratio of the element, but not on the mesh-size h.

We will also use a lifting operator $P_\ell:\mathbb{P}_n(\ell)\to\mathbb{P}_n(\omega_\ell)$ such that, for all $s\in\mathbb{P}_n(\ell)$, $P_\ell(s)|_\ell = s$ and

$$\|b_\ell P_\ell(s)\|_{0,\omega_\ell} \leqslant C h_\ell\,|b_\ell P_\ell(s)|_{1,\omega_\ell} \leqslant C' h_\ell^{\frac{1}{2}}\,\|s\|_{0,\ell}, \tag{4.3}$$

h_ℓ being the diameter of ℓ (see Verfürth (1998) for a construction). Finally, for $\boldsymbol{s}=(s_1,\dots,s_N)\in\mathbb{P}_n(\ell)^N$, we denote

$$\boldsymbol{P}_\ell(\boldsymbol{s}) := (P_\ell(s_1),\dots,P_\ell(s_N)).$$

4.2 *The estimator*

By integrating by parts, we arrive at the following residual equation:

$$\begin{aligned}
&\mathscr{B}\left(((\boldsymbol{u}-\boldsymbol{u}_h,\varphi-\varphi_h),p-p_h),((\boldsymbol{v},\psi),q)\right)\\
&\quad=\int_{\Omega_S}\boldsymbol{f}_S\cdot\boldsymbol{v}+\int_{\Gamma_N}\boldsymbol{g}\cdot\boldsymbol{v}+\int_{\Omega_F}\boldsymbol{f}_F\cdot\nabla\psi-\int_{\Omega_S}\boldsymbol{\sigma}(\boldsymbol{u}_h):\boldsymbol{\varepsilon}(\boldsymbol{v})-\int_{\Omega_F}\nabla\psi\cdot\nabla p_h+\int_{\Gamma_I}p_h\boldsymbol{v}\cdot\boldsymbol{n}\\
&\qquad-\int_{\Omega_F}\nabla\varphi_h\cdot\nabla q+\int_{\Gamma_I}q\boldsymbol{u}_h\cdot\boldsymbol{n}+\int_{\Omega_F}\frac{1}{\rho_F c^2}\,p_h q\\
&\quad=\sum_{K\in\mathscr{T}_h^S}\int_K \boldsymbol{R}_K^{\boldsymbol{u}}\cdot\boldsymbol{v}+\sum_{\ell\in\mathscr{E}_h^S}\int_\ell \boldsymbol{J}_\ell^{\boldsymbol{u}}\cdot\boldsymbol{v}+\sum_{K\in\mathscr{T}_h^F}\int_K\left(R_K^p\psi+R_K^\varphi q\right)+\sum_{\ell\in\mathscr{E}_h^F}\int_\ell\left(J_\ell^p\psi+J_\ell^\varphi q\right),
\end{aligned}\tag{4.4}$$

for all $((\boldsymbol{v},\psi),q)\in\mathscr{X}\times\mathscr{M}$, where the element and edge (face) residuals are defined as follows:

$$\boldsymbol{R}_K^{\boldsymbol{u}} := \boldsymbol{f}_S|_K+\operatorname{div}\boldsymbol{\sigma}(\boldsymbol{u}_h|_K), \qquad \boldsymbol{J}_\ell^{\boldsymbol{u}} := \begin{cases} [\![\boldsymbol{\sigma}(\boldsymbol{u}_h)\boldsymbol{n}_\ell]\!]_\ell, & \text{if } \ell\in\widetilde{\mathscr{E}}_h^S,\\ [-\boldsymbol{\sigma}(\boldsymbol{u}_h)\boldsymbol{\nu}+\boldsymbol{g}]|_\ell, & \text{if } \ell\in\mathscr{E}_h^N,\\ [\boldsymbol{\sigma}(\boldsymbol{u}_h)\boldsymbol{n}+p_h\boldsymbol{n}]|_\ell, & \text{if } \ell\in\mathscr{E}_h^I,\\ \boldsymbol{0}, & \text{if } \ell\in\mathscr{E}_h^D,\end{cases}$$

$$R_K^p := -\operatorname{div}(\boldsymbol{f}_F|_K)+\Delta(p_h|_K), \qquad J_\ell^p := \begin{cases} \left[\!\left[-\frac{\partial p_h}{\partial \boldsymbol{n}_\ell}+\boldsymbol{f}_F\cdot\boldsymbol{n}_\ell\right]\!\right]_\ell, & \text{if } \ell\in\widetilde{\mathscr{E}}_h^F,\\ \left(-\frac{\partial p_h}{\partial \boldsymbol{n}}+\boldsymbol{f}_F\cdot\boldsymbol{n}\right)\Big|_\ell, & \text{if } \ell\in\mathscr{E}_h^I,\end{cases}$$

$$R_K^{\varphi} := \Delta(\varphi_h|_K) + \frac{1}{\rho_F c^2}\, p_h|_K, \qquad J_\ell^{\varphi} := \begin{cases} \left[\!\left[\frac{\partial \varphi_h}{\partial \boldsymbol{n}_\ell} \right]\!\right]_\ell, & \text{if } \ell \in \widetilde{\mathscr{E}}_h^F, \\ \left(\frac{\partial \varphi_h}{\partial \boldsymbol{n}} + \boldsymbol{u}_h \cdot \boldsymbol{n} \right)\Big|_\ell, & \text{if } \ell \in \mathscr{E}_h^I, \end{cases}$$

where $\boldsymbol{n}_\ell$ denotes a unit vector normal to $\ell \in \widetilde{\mathscr{E}}_h^S \cup \widetilde{\mathscr{E}}_h^F$ and $[\![\cdot]\!]_\ell$ the jump across the edge (face).

The residual equation above leads us to define the following residual a posteriori error estimator:

$$\eta^2 := \sum_{K \in \mathscr{T}_h^S} (\eta_K^{\boldsymbol{u}})^2 + \sum_{K \in \mathscr{T}_h^F} \left[(\eta_K^p)^2 + (\eta_K^{\varphi})^2 \right], \tag{4.5}$$

where

$$\begin{aligned}
(\eta_K^{\boldsymbol{u}})^2 &:= h_K^2 \, \|R_K^{\boldsymbol{u}}\|_{0,K}^2 + \sum_{\ell \in \mathscr{E}_K} \delta_\ell h_\ell \, \|J_\ell^{\boldsymbol{u}}\|_{0,\ell}^2, \qquad K \in \mathscr{T}_h^S, \\
(\eta_K^p)^2 &:= h_K^2 \, \|R_K^p\|_{0,K}^2 + \sum_{\ell \in \mathscr{E}_K} \delta_\ell h_\ell \, \|J_\ell^p\|_{0,\ell}^2, \qquad K \in \mathscr{T}_h^F, \\
(\eta_K^{\varphi})^2 &:= h_K^2 \, \|R_K^{\varphi}\|_{0,K}^2 + \sum_{\ell \in \mathscr{E}_K} \delta_\ell h_\ell \, \|J_\ell^{\varphi}\|_{0,\ell}^2, \qquad K \in \mathscr{T}_h^F,
\end{aligned}$$

with

$$\delta_\ell = \begin{cases} \frac{1}{2}, & \text{if } \ell \in \widetilde{\mathscr{E}}_h^S \cup \widetilde{\mathscr{E}}_h^F, \\ 1, & \text{if } \ell \in \mathscr{E}_h^N \cup \mathscr{E}_h^D \cup \mathscr{E}_h^I. \end{cases}$$

We prove in the following theorem the efficiency and reliability of this estimator.

THEOREM 4.1 There exist positive constants C_1 and C_2, not depending on h or c, such that

$$\|\boldsymbol{u} - \boldsymbol{u}_h\|_{1,\Omega_S} + |\varphi - \varphi_h|_{1,\Omega_F} + \|p - p_h\|_{1,\Omega_F} \leqslant C_1 \eta \tag{4.6}$$

and

$$\eta_K^{\boldsymbol{u}} \leqslant C_2 \left(|\boldsymbol{u} - \boldsymbol{u}_h|_{1,\omega_K^S} + \delta_K p \right) \qquad \forall K \in \mathscr{T}_h^S, \tag{4.7}$$

$$\eta_K^p \leqslant C_2 \, |p - p_h|_{1,\omega_K^F} \qquad \forall K \in \mathscr{T}_h^F, \tag{4.8}$$

$$\eta_K^{\varphi} \leqslant C_2 \left(|\varphi - \varphi_h|_{1,\omega_K^F} + \frac{h_K}{\rho_F c^2} \|p - p_h\|_{0,\omega_K^F} + \delta_K \boldsymbol{u} \right) \qquad \forall K \in \mathscr{T}_h^F, \tag{4.9}$$

where

$$\delta_K p := \begin{cases} 0, & \text{if } \mathscr{E}_K \cap \mathscr{E}_h^I = \emptyset, \\ \sum_{\ell \in \mathscr{E}_K \cap \mathscr{E}_h^I} \left(\|p - p_h\|_{0,K_\ell^F} + h_K \, |p - p_h|_{1,K_\ell^F} \right), & \text{if } \mathscr{E}_K \cap \mathscr{E}_h^I \neq \emptyset, \end{cases}$$

$$\delta_K \boldsymbol{u} := \begin{cases} 0, & \text{if } \mathscr{E}_K \cap \mathscr{E}_h^I = \emptyset, \\ \sum_{\ell \in \mathscr{E}_K \cap \mathscr{E}_h^I} \left(\|\boldsymbol{u} - \boldsymbol{u}_h\|_{0,K_\ell^S} + h_K \, |\boldsymbol{u} - \boldsymbol{u}_h|_{1,K_\ell^S} \right), & \text{if } \mathscr{E}_K \cap \mathscr{E}_h^I \neq \emptyset. \end{cases}$$

Proof. For $((\boldsymbol{v}, \psi), q) \in \mathscr{X} \times \mathscr{M}$, let $\boldsymbol{v}_h$, ψ_h and q_h be the Scott-Zhang interpolants of $\boldsymbol{v}$, ψ and q, respectively. Then, using the residual equation (4.4), the Galerkin orthogonality, Cauchy-Schwarz's inequality and the properties of the interpolant we obtain:

$$\begin{aligned}
&\mathscr{B}\left(((\boldsymbol{u}-\boldsymbol{u}_h,\varphi-\varphi_h),p-p_h),((\boldsymbol{v},\psi),q)\right)\\
&\quad=\mathscr{B}\left(((\boldsymbol{u}-\boldsymbol{u}_h,\varphi-\varphi_h),p-p_h),((\boldsymbol{v}-\boldsymbol{v}_h,\psi-\psi_h),q-q_h)\right)\\
&\quad=\sum_{K\in\mathscr{T}_h^S}\int_K R_K^{\boldsymbol{u}}\cdot(\boldsymbol{v}-\boldsymbol{v}_h)+\sum_{\ell\in\mathscr{E}_h^S}\int_\ell J_\ell^{\boldsymbol{u}}\cdot(\boldsymbol{v}-\boldsymbol{v}_h)+\sum_{K\in\mathscr{T}_h^F}\int_K\left[R_K^p(\psi-\psi_h)+R_K^{\varphi}(q-q_h)\right]\\
&\qquad+\sum_{\ell\in\mathscr{E}_h^F}\int_\ell\left[J_\ell^p(\psi-\psi_h)+J_\ell^{\varphi}(q-q_h)\right]\\
&\quad\leqslant C\Bigg[\sum_{K\in\mathscr{T}_h^S}h_K^2\,\|R_K^{\boldsymbol{u}}\|_{0,K}^2+\sum_{\ell\in\mathscr{E}_h^S}h_\ell\,\|J_\ell^{\boldsymbol{u}}\|_{0,\ell}^2+\sum_{K\in\mathscr{T}_h^F}h_K^2\left(\left\|R_K^p\right\|_{0,K}^2+\left\|R_K^{\varphi}\right\|_{0,K}^2\right)\\
&\qquad\quad+\sum_{\ell\in\mathscr{E}_h^F}h_\ell\left(\left\|J_\ell^p\right\|_{0,\ell}^2+\left\|J_\ell^{\varphi}\right\|_{0,\ell}^2\right)\Bigg]^{\frac12}\|((\boldsymbol{v},\psi),q)\|_{\mathscr{X}\times\mathscr{M}}\,.
\end{aligned}$$

Hence, using (2.22) we arrive at

$$\begin{aligned}
&\|\boldsymbol{u}-\boldsymbol{u}_h\|_{1,\Omega_S}+|\varphi-\varphi_h|_{1,\Omega_F}+\|p-p_h\|_{1,\Omega_F}\\
&\qquad\leqslant C_{\mathscr{B}}\sup_{((\boldsymbol{v},\psi),q)\in\mathscr{X}\times\mathscr{M}\setminus\{\boldsymbol{0}\}}\frac{\mathscr{B}\left(((\boldsymbol{u}-\boldsymbol{u}_h,\varphi-\varphi_h),p-p_h),((\boldsymbol{v},\psi),q)\right)}{\|((\boldsymbol{v},\psi),q)\|_{\mathscr{X}\times\mathscr{M}}}\\
&\qquad\leqslant C_1\,\eta\,.
\end{aligned}$$

Thus we conclude the reliability estimate (4.6).

To prove the efficiency, we will treat each term of the estimator separately.

1. For all $K\in\mathscr{T}_h^S$
$$h_K^2\,\|R_K^{\boldsymbol{u}}\|_{0,K}^2\leqslant C\,|\boldsymbol{u}-\boldsymbol{u}_h|_{1,K}^2\,. \tag{4.10}$$
Let $\boldsymbol{v}_K:=b_K R_K^{\boldsymbol{u}}$. Taking $((\boldsymbol{v},\psi),q)=((\boldsymbol{v}_K,0),0)$ in (4.4) and using (4.1) and an inverse inequality, we arrive at
$$\begin{aligned}
\|R_K^{\boldsymbol{u}}\|_{0,K}^2&\leqslant C\int_K R_K^{\boldsymbol{u}}\cdot\boldsymbol{v}_K=C\int_K\boldsymbol{\sigma}(\boldsymbol{u}-\boldsymbol{u}_h):\boldsymbol{\varepsilon}(\boldsymbol{v}_K)\leqslant C\,|\boldsymbol{u}-\boldsymbol{u}_h|_{1,K}\,|\boldsymbol{v}_K|_{1,K}\\
&\leqslant C h_K^{-1}\,|\boldsymbol{u}-\boldsymbol{u}_h|_{1,K}\,\|R_K^{\boldsymbol{u}}\|_{0,K}\,,
\end{aligned}$$
which yields (4.10).

2. For all $\ell\in\mathscr{E}_h^S$
$$h_\ell\,\|J_\ell^{\boldsymbol{u}}\|_{0,\ell}^2\leqslant C\begin{cases}|\boldsymbol{u}-\boldsymbol{u}_h|_{1,\omega_\ell^S}^2\,, & \text{if } \ell\in\widetilde{\mathscr{E}}_h^S\cup\mathscr{E}_h^N,\\ |\boldsymbol{u}-\boldsymbol{u}_h|_{1,\omega_\ell^S}^2+\|p-p_h\|_{0,K_\ell^F}^2+h_K^2\,|p-p_h|_{1,K_\ell^F}^2\,, & \text{if } \ell\in\mathscr{E}_h^I.\end{cases} \tag{4.11}$$
First, consider $\ell\in\widetilde{\mathscr{E}}_h^S\cup\mathscr{E}_h^N$. Defining $\boldsymbol{v}_\ell:=b_\ell\boldsymbol{P}_\ell(J_\ell^{\boldsymbol{u}})$, using (4.2), $((\boldsymbol{v}_\ell,0),0)$ in the residual

equation (4.4), and (4.3), we obtain

$$\begin{aligned}
\|J_\ell^{\boldsymbol{u}}\|_{0,\ell}^2 &\leqslant C\int_\ell J_\ell^{\boldsymbol{u}}\cdot\boldsymbol{v}_\ell = C\left[\int_{\omega_\ell^S}\boldsymbol{\sigma}(\boldsymbol{u}-\boldsymbol{u}_h):\boldsymbol{\varepsilon}(\boldsymbol{v}_\ell)-\sum_{K\subset\omega_\ell^S}\int_K R_K^{\boldsymbol{u}}\cdot\boldsymbol{v}_\ell\right]\\
&\leqslant C\left(|\boldsymbol{u}-\boldsymbol{u}_h|_{1,\omega_\ell^S}|\boldsymbol{v}_\ell|_{1,\omega_\ell^S}+\sum_{K\subset\omega_\ell^S}\|R_K^{\boldsymbol{u}}\|_{0,K}\|\boldsymbol{v}_\ell\|_{0,K}\right)\\
&\leqslant C\left(|\boldsymbol{u}-\boldsymbol{u}_h|_{1,\omega_\ell^S}h_\ell^{-\frac12}\|J_\ell^{\boldsymbol{u}}\|_{0,\ell}+\sum_{K\subset\omega_\ell^S}h_\ell^{\frac12}\|R_K^{\boldsymbol{u}}\|_{0,K}\|J_\ell^{\boldsymbol{u}}\|_{0,\ell}\right)\\
&\leqslant C\left(|\boldsymbol{u}-\boldsymbol{u}_h|_{1,\omega_\ell^S}^2+\sum_{K\subset\omega_\ell^S}h_K^2\|R_K^{\boldsymbol{u}}\|_{0,K}^2\right)^{\frac12}h_\ell^{-\frac12}\|J_\ell^{\boldsymbol{u}}\|_{0,\ell}.
\end{aligned}$$

Therefore, the first part of (4.11) follows from (4.10).

Next, consider $\ell\in\mathscr{E}_h^I$. Let $K:=K_\ell^S$ and $\boldsymbol{v}_\ell:=b_\ell\boldsymbol{P}_\ell(J_\ell^{\boldsymbol{u}})$, where the extension is taken in $\omega_\ell^S=K$. Proceeding as above we arrive at

$$\begin{aligned}
\|J_\ell^{\boldsymbol{u}}\|_{0,\ell}^2 &\leqslant C\int_\ell J_\ell^{\boldsymbol{u}}\cdot\boldsymbol{v}_\ell = C\left[\int_K\boldsymbol{\sigma}(\boldsymbol{u}-\boldsymbol{u}_h):\boldsymbol{\varepsilon}(\boldsymbol{v}_\ell)-\int_\ell(p-p_h)\boldsymbol{v}_\ell\cdot\boldsymbol{n}-\int_K R_K^{\boldsymbol{u}}\cdot\boldsymbol{v}_\ell\right]\\
&\leqslant C\left(|\boldsymbol{u}-\boldsymbol{u}_h|_{1,K}|\boldsymbol{v}_\ell|_{1,K}+\|p-p_h\|_{0,\ell}\|\boldsymbol{v}_\ell\|_{0,\ell}+\|R_K^{\boldsymbol{u}}\|_{0,K}\|\boldsymbol{v}_\ell\|_{0,K}\right)\\
&\leqslant C\left(|\boldsymbol{u}-\boldsymbol{u}_h|_{1,K}^2+h_\ell\|p-p_h\|_{0,\ell}^2+h_K^2\|R_K^{\boldsymbol{u}}\|_{0,K}^2\right)^{\frac12}h_\ell^{-\frac12}\|J_\ell^{\boldsymbol{u}}\|_{0,\ell},
\end{aligned}$$

and hence

$$h_\ell\|J_\ell^{\boldsymbol{u}}\|_{0,\ell}^2\leqslant C\left(|\boldsymbol{u}-\boldsymbol{u}_h|_{1,K}^2+h_\ell\|p-p_h\|_{0,\ell}^2+h_K^2\|R_K^{\boldsymbol{u}}\|_{0,K}^2\right).$$

Finally, we use the local trace inequality

$$\|p-p_h\|_{0,\ell}^2\leqslant C\left(h_\ell^{-1}\|p-p_h\|_{0,K_\ell^F}^2+h_\ell|p-p_h|_{1,K_\ell^F}^2\right) \tag{4.12}$$

and (4.10) to obtain the second part of (4.11). Thus, (4.7) follows from (4.10) and (4.11).

3. For all $K\in\mathscr{T}_h^F$

$$h_K^2\left\|R_K^p\right\|_{0,K}^2\leqslant C|p-p_h|_{1,K}^2, \tag{4.13}$$

and for all $\ell\in\mathscr{E}_h^F$

$$h_\ell\left\|J_\ell^p\right\|_{0,\ell}^2\leqslant C|p-p_h|_{1,\omega_\ell^F}^2. \tag{4.14}$$

The proofs of (4.13) and (4.14) are essentially identical to those of (4.10) and the first estimate in (4.11), respectively. Thus (4.8) follows.

4. For all $K\in\mathscr{T}_h^F$

$$h_K^2\left\|R_K^\varphi\right\|_{0,K}^2\leqslant C\left[|\varphi-\varphi_h|_{1,K}^2+\frac{h_K^2}{(\rho_F c^2)^2}\|p-p_h\|_{0,K}^2\right], \tag{4.15}$$

and for all $\ell \in \mathscr{E}_h^F$

$$h_\ell \left\| J_\ell^\varphi \right\|_{0,\ell}^2 \leqslant C \begin{cases} |\varphi - \varphi_h|_{1,\omega_\ell^F}^2 + \frac{h_K^2}{(\rho_F c^2)^2} \|p - p_h\|_{0,\omega_\ell^F}^2 , & \text{if } \ell \in \widetilde{\mathscr{E}}_h^F, \\ |\varphi - \varphi_h|_{1,\omega_\ell^F}^2 + \frac{h_K^2}{(\rho_F c^2)^2} \|p - p_h\|_{0,\omega_\ell^F}^2 & \\ \qquad + \|\boldsymbol{u} - \boldsymbol{u}_h\|_{0,K_\ell^S}^2 + h_K^2 |\boldsymbol{u} - \boldsymbol{u}_h|_{1,K_\ell^S}^2 , & \text{if } \ell \in \mathscr{E}_h^I. \end{cases} \tag{4.16}$$

The proof of (4.15) is essentially identical to that of (4.10), whereas, for $\ell \in \widetilde{\mathscr{E}}_h^F$, (4.16) follows by using the same arguments as in (4.11). Thus, there only remains to consider $\ell \in \mathscr{E}_h^I$. Let $K := K_\ell^F$ and $q_\ell = b_\ell P_\ell(J_\ell^\varphi)$, where the extension is taken in $\omega_\ell^F = K$. Using $((\boldsymbol{v},\psi),q) = ((\boldsymbol{0},0),q_\ell)$ in (4.4), we have

$$\begin{aligned} \left\| J_\ell^\varphi \right\|_{0,\ell}^2 &\leqslant C \int_\ell J_\ell^\varphi q_\ell = C \left[\int_K \nabla(\varphi - \varphi_h) \cdot \nabla q_\ell - \int_\ell (\boldsymbol{u} - \boldsymbol{u}_h) \cdot \boldsymbol{n} q_\ell + \int_K \frac{1}{\rho_F c^2} (p - p_h) q_\ell - \int_K R_K^\varphi q_\ell \right] \\ &\leqslant C \left[|\varphi - \varphi_h|_{1,K}^2 + h_\ell \|\boldsymbol{u} - \boldsymbol{u}_h\|_{0,\ell}^2 + \frac{h_K^2}{(\rho_F c^2)^2} \|p - p_h\|_{0,K}^2 + h_K^2 \left\| R_K^\varphi \right\|_{0,K}^2 \right]^{\frac{1}{2}} h_\ell^{-\frac{1}{2}} \left\| J_\ell^\varphi \right\|_{0,\ell} , \end{aligned}$$

which using (4.15) leads to

$$h_\ell \left\| J_\ell^\varphi \right\|_{0,\ell}^2 \leqslant C \left[|\varphi - \varphi_h|_{1,K}^2 + h_\ell \|\boldsymbol{u} - \boldsymbol{u}_h\|_{0,\ell}^2 + \frac{h_K^2}{(\rho_F c^2)^2} \|p - p_h\|_{0,K}^2 \right].$$

Therefore, (4.16) follows by using a local trace inequality for $\boldsymbol{u} - \boldsymbol{u}_h$ similar to (4.12). The proof is finished by noting that (4.9) follows from (4.15) and (4.16).

□

REMARK 4.1 The coupling terms $\delta_K p$ and $\delta_K \boldsymbol{u}$, as well as $\frac{h_K}{\rho_F c^2} \|p - p_h\|_{0,\omega_K^F}$, are very likely negligible in the reliability estimates (4.7) and (4.9). Indeed, all of them involve either the seminorm $|\cdot|_{1,K}$ of some error times h_K, or the norm $\|\cdot\|_{0,K}$. (Recall that, according to Theorem 3.2, the norm $\|\cdot\|_0$ of the errors are globally of higher order than the corresponding seminorm $|\cdot|_1$.)

5. Numerical Experiments

In this section we present three series of numerical experiments illustrating the theoretical results of the previous sections, the performance of the method and that of an adaptive scheme based on the a posteriori error estimator.

5.1 *A problem with a known analytical solution*

The aim of this first test is to validate the computational code and to confirm the theoretical convergence results. To do this, we adopt the configuration shown in Fig. 2.

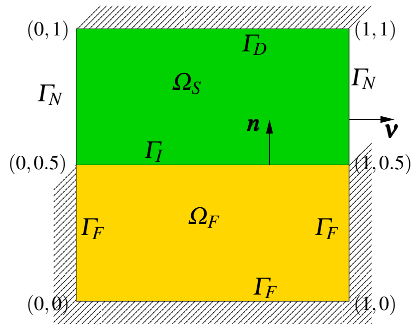

FIG. 2. Problem with analytical solution: sketch of the domains.

A piece Γ_F of the fluid domain boundary is taken as a perfectly rigid wall, which leads to the boundary condition $\frac{\partial \varphi}{\partial \boldsymbol{n}} = 0$ on Γ_F. The other boundary conditions remain as above, $\boldsymbol{u} = \mathbf{0}$ on Γ_D and $\boldsymbol{\sigma\nu} = \boldsymbol{g}$ on Γ_N. We set $\rho_F = 1$, $c = 1$, $\lambda = 0.5$ and $\mu = 0.25$. The data $\boldsymbol{f}_F$, $\boldsymbol{f}_S$ and $\boldsymbol{g}$ are chosen so that the exact solution to the problem is given by

$$\boldsymbol{u}(x,y) = \begin{bmatrix} 0 \\ y^2(y-1) \end{bmatrix}, \qquad \varphi(x,y) = \frac{y^4}{4} - \frac{y^3}{3} + \frac{7}{960}, \qquad p(x,y) = -(3y^2 - 2y).$$

REMARK 5.1 We have taken the physical parameters so that $\lambda + 2\mu = \rho_F c^2$, to ensure that the transmission condition (2.5) is satisfied.

REMARK 5.2 The analysis carried out in the previous sections may be adapted, with minor modifications, to cover this problem too, so that all the results from Sections 2–4 hold. In particular, since the solution of this test is infinitely smooth, according to Theorem 3.1, the H^1 norm of the errors must be $\mathcal{O}(h)$. Furthermore, the constants s and t in Theorem 3.2 are both equal to 1, so that the L^2 norm of the errors must be $\mathcal{O}(h^2)$.

We depict in Figs. 3 and 5 the convergence of the error in each variable on uniform meshes as h tends to 0. The figures show a perfect agreement with the theoretical results.

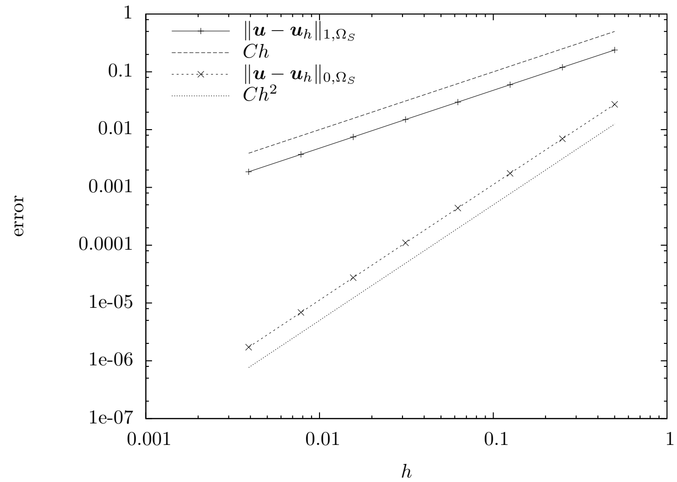

FIG. 3. Problem with analytical solution: convergence history for $\|\boldsymbol{u}-\boldsymbol{u}_h\|_{0,\Omega_S}$ and $\|\boldsymbol{u}-\boldsymbol{u}_h\|_{1,\Omega_S}$ with uniform meshes.

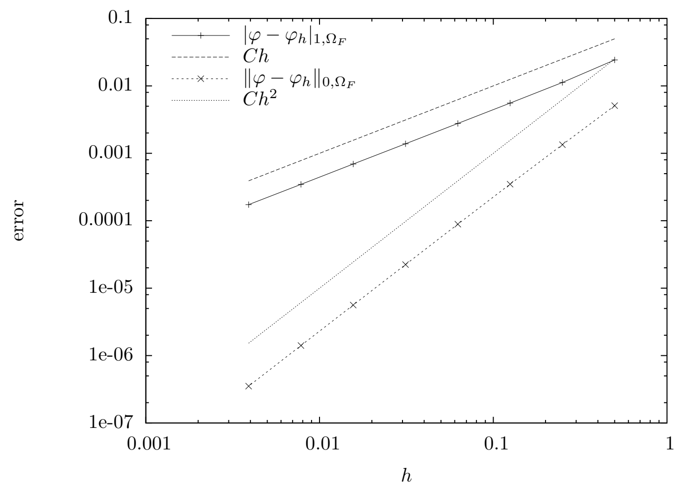

FIG. 4. Problem with analytical solution: convergence history for $\|\varphi-\varphi_h\|_{0,\Omega_F}$ and $|\varphi-\varphi_h|_{1,\Omega_F}$ with uniform meshes.

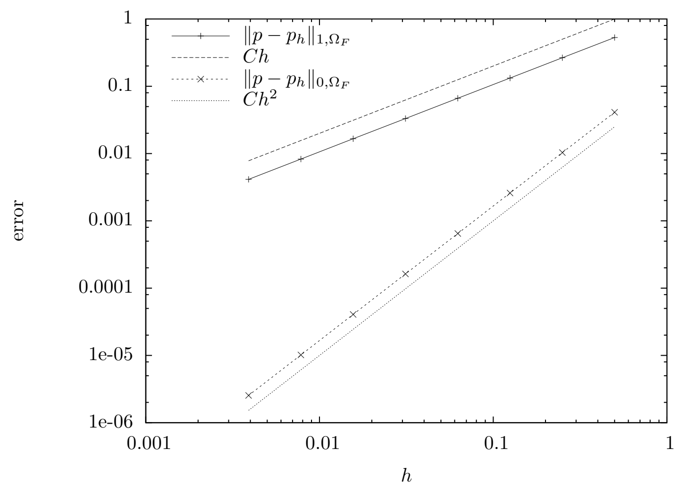

FIG. 5. Problem with analytical solution: convergence history for $\|p-p_h\|_{0,\Omega_F}$ and $\|p-p_h\|_{1,\Omega_F}$ with uniform meshes.

Next, denoting

$$\eta^{\boldsymbol{u}} := \left[\sum_{K\in\mathscr{T}_h^S} (\eta_K^{\boldsymbol{u}})^2\right]^{\frac{1}{2}}, \qquad \eta^{p} := \left[\sum_{K\in\mathscr{T}_h^F} (\eta_K^{p})^2\right]^{\frac{1}{2}}, \qquad \eta^{\varphi} := \left[\sum_{K\in\mathscr{T}_h^F} (\eta_K^{\varphi})^2\right]^{\frac{1}{2}},$$

we show in Table 1 the effectivity indices for each variable:

$$\theta^{\boldsymbol{u}} := \frac{\eta^{\boldsymbol{u}}}{\|\boldsymbol{u}-\boldsymbol{u}_h\|_{1,\Omega_S}}, \qquad \theta^{\varphi} := \frac{\eta^{\varphi}}{|\varphi-\varphi_h|_{1,\Omega_F}}, \qquad \theta^{p} := \frac{\eta^{p}}{\|p-p_h\|_{1,\Omega_F}},$$

and the global effectivity index

$$\theta := \frac{\eta}{\sqrt{\|\boldsymbol{u}-\boldsymbol{u}_h\|_{1,\Omega_S}^2 + |\varphi-\varphi_h|_{1,\Omega_F}^2 + \|p-p_h\|_{1,\Omega_F}^2}}.$$

Table 1. Problem with analytical solution: effectivity indices on uniform meshes.

d.o.f.	$\theta^{\boldsymbol{u}}$	θ^{φ}	θ^{p}	θ
32	2.5567	2.5581	3.3067	3.1921
92	2.8298	3.5696	3.6714	3.5435
308	2.9748	3.8921	3.8398	3.7082
1124	3.0487	3.9977	3.9209	3.7880
4292	3.0857	4.0352	3.9606	3.8273
16772	3.1042	4.0499	3.9804	3.8468
66308	3.1134	4.0563	3.9902	3.8565
283684	3.1180	4.0592	3.9951	3.8613

Note that all the indices converge towards constants, even though this fact is not predicted by the theory presented in the last section. In this table and thereafter, d.o.f. denote the total number of degrees of freedom for the three variables.

5.2 *An L-shaped vessel filled with a compressible fluid*

Next, we test the method in a problem without a known analytical solution. In this test (and in the following one), we are particularly interested in assessing the performance of an adaptive procedure guided by the error indicators

$$\eta_K := \begin{cases} \eta_K^{\boldsymbol{u}}, & K \in \mathscr{T}_h^S, \\ \left[(\eta_K^p)^2 + (\eta_K^\varphi)^2\right]^{\frac{1}{2}}, & K \in \mathscr{T}_h^F. \end{cases}$$

The basic scheme of the adaptive procedure is as follows:

1. Solve (3.1)–(3.2) in an initial mesh $\mathscr{T}_0 := \mathscr{T}_0^S \cup \mathscr{T}_0^F$ and compute $\eta_K\ \forall K \in \mathscr{T}_0$.
2. If $\eta_K \geqslant \delta \max_{K' \in \mathscr{T}_0} \eta_{K'}$ (where $0 < \delta < 1$ is fixed in advance), then K is subdivided.
3. The process is repeated until η is smaller than a prescribed tolerance.

The meshes are generated with `Triangle` (cf. Shewchuck (2002)) and we have implemented the case in which the meshes for the fluid and the solid match on the common interface. We have used the value $\delta = 0.75$ in all the experiments.

The domain and boundary conditions are described in Fig. 6 (left). We have taken all the physical parameters set to one: $\lambda = \mu = \rho_S = \rho_F = c = 1$. The external forces have been taken as follows:

- $\boldsymbol{f}_S = (0, -1)$,
- $\boldsymbol{f}_F = \nabla(r^{\frac{2}{3}} \sin \frac{2}{3}\theta)$, where $r := |\boldsymbol{x} - \boldsymbol{x}_0|$, and θ and $\boldsymbol{x}_0$ are shown in Fig. 6 (left).

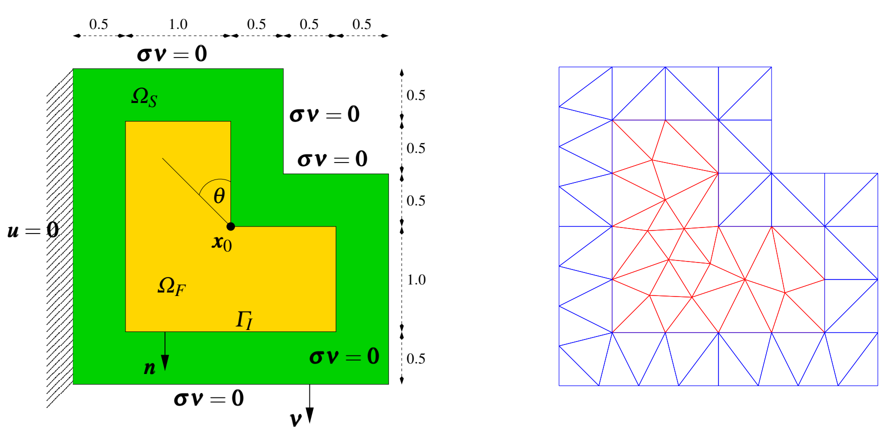

FIG. 6. Sketch of the L-shaped domains (left) and initial mesh (right).

Several singularities appear in this case, because of the reentrant angles of Ω_S and Ω_F, the definition of $\boldsymbol{f}_F$ and the change on the boundary conditions. In Fig. 6 (right) we depict the initial mesh used for this test and in Fig. 7 the adapted meshes after 10 and 20 iterations.

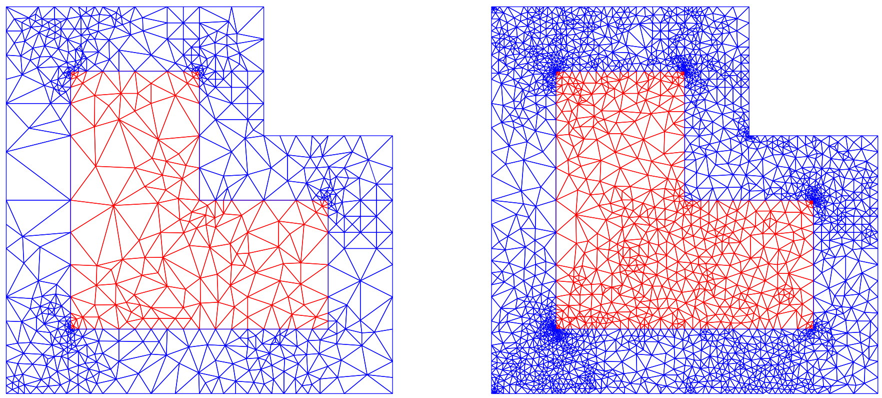

FIG. 7. L-shaped domains: adapted meshes after 15 (left) and 25 iterations (right).

It can be seen that the indicator is able to capture all the singularities in the fluid and the solid domains. In fact, Fig. 8 shows zooms of a highly refined adapted mesh in the vicinity of reentrant angles of the fluid (left) and the solid (right) domains.

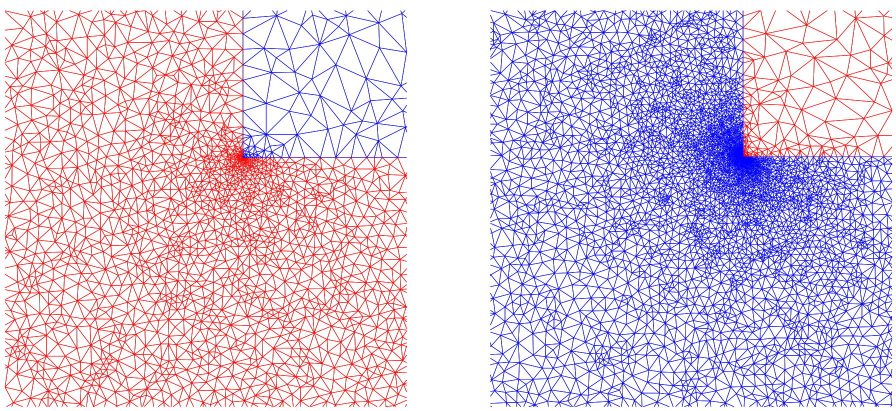

FIG. 8. L-shaped domains: zoom of an adapted mesh at reentrant angles of the fluid (left) and solid (right) domains.

We do not report error curves in this case, because no analytical solution is available. Instead, we depict in Fig. 9 the estimated global error η (cf. (4.5)) versus the total number of degrees of freedom for adapted and uniformly refined meshes.

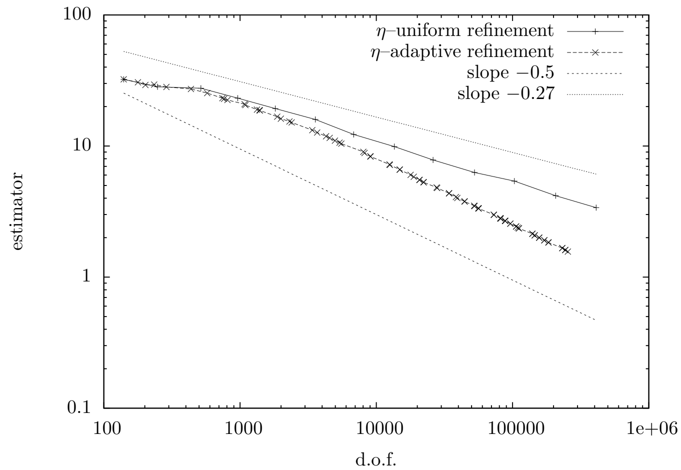

FIG. 9. L-shaped domains: convergence history for η vs. d.o.f. with uniform and adaptively refined meshes.

Let us remark that since η is an estimator of $(\|\boldsymbol{u}-\boldsymbol{u}_h\|^2_{1,\Omega_S}+|\varphi-\varphi_h|^2_{1,\Omega_F}+\|p-p_h\|^2_{1,\Omega_F})^{1/2}$ and in this case $(\|\boldsymbol{u}\|^2_{1,\Omega_S}+|\varphi|^2_{1,\Omega_F}+\|p\|^2_{1,\Omega_F})^{1/2}\approx 112$, the estimated errors shown in Fig 9 correspond to relative errors ranging from 30% to 3% for the uniform meshes and from 30% to 1.4% for the adaptively refined ones.

We have included in Fig. 9 two lines with slopes -0.27 and -0.5. The first one corresponds to the theoretical order of convergence for the error with uniform meshes. The second one corresponds to the optimal order that could be attained with piecewise linear elements. The orders of convergence for the depicted estimated error curves have been also computed by means of a least squares fitting which yield values -0.287 and -0.498, respectively. Both are very close to the expected ones for the error.

Because of the equivalence proved between the estimated and the actual global errors, both have the same asymptotic dependence on the total number of degrees of freedom. Therefore, the estimated error curve indicates that the error itself has to attain an optimal order, too, when the adaptive meshes are used. This yields some evidence on the fact that the adaptively created meshes should be close to the optimal ones.

5.3 *A vessel filled with an ideal incompressible fluid*

Finally, we test the method with a fluid which is modeled as perfectly incompressible. We have used the same physical parameters as in the previous test, except for the sound speed which has been taken $c=\infty$; namely, $d(p,q)\equiv 0$ in (3.1)–(3.2) (cf. Remark 2.2).

The domain and boundary conditions are described in Fig. 10 (left) and we have taken $\boldsymbol{f}_S=(0,-1)$ and $\boldsymbol{f}_F=(0,-1)$, as well.

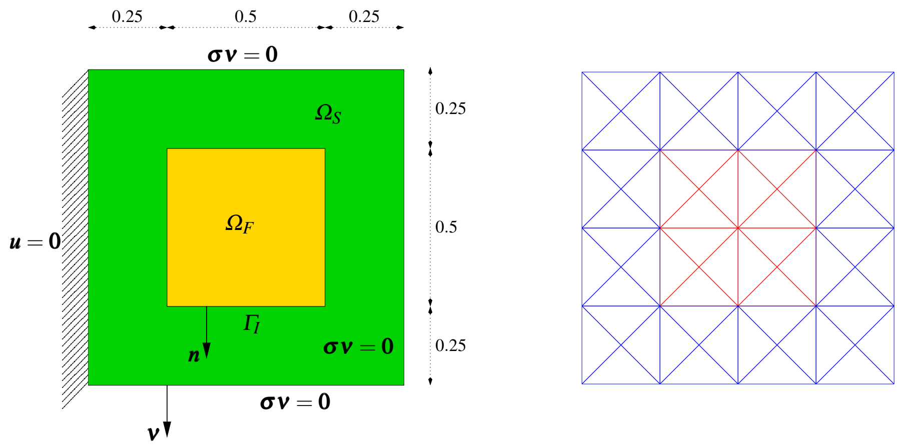

FIG. 10. Incompressible fluid: sketch of the domains (left) and initial mesh (right).

In Fig. 10 (right) we depict the initial mesh used for this test and in Fig. 11 the adapted meshes after 7 and 15 iterations.

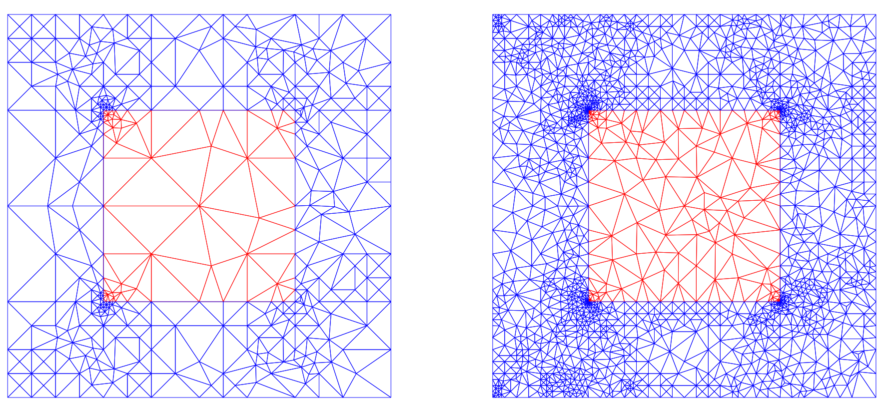

FIG. 11. Incompressible fluid: adapted meshes after 7 (left) and 15 iterations (right).

We observe that the indicator is able to capture all the singularities: one at each reentrant angle of Ω_S and other two at the top and bottom left corners (because of the change on the boundary conditions). Since the fluid domain is convex, no singularity appears in the fluid. This is recognized by the estimator, since the elements in Ω_F are refined only to preserve the compatibility of the meshes on the fluid-solid interface. This can be clearly seen in Fig. 12, which shows a zoom of a highly refined adapted mesh in the vicinity of one of the reentrant angles.

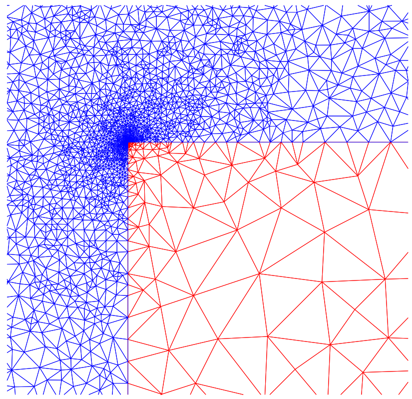

FIG. 12. Incompressible fluid: zoom of an adapted mesh at a reentrant angle.

We depict in Fig. 13 the estimated global error η versus the total number of degrees of freedom.

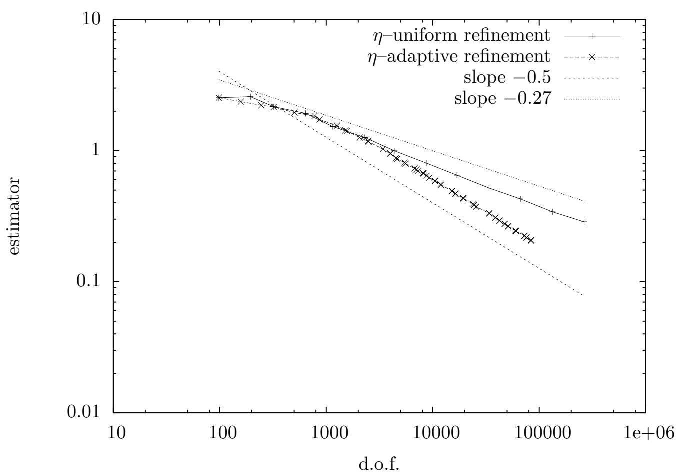

FIG. 13. Incompressible fluid: convergence history for η vs. d.o.f. with uniform and adaptively refined meshes.

Once more, we have included in Fig. 13 two lines with slopes -0.27 and -0.5, which correspond to the theoretical order of convergence for the error with uniform meshes and the optimal order attainable with piecewise linear elements, respectively. It can be seen from this figure that, for sufficiently refined meshes, the adaptive scheme yields an optimal order of convergence, again. In fact, the orders of convergence for the depicted estimated error curves computed by a least squares fitting are in this case -0.288 and -0.499, respectively.

Let us finally remark, that the performance of the method is not affected by the fact that the fluid is incompressible.

A. Appendix: A nonlinear elastic material

This section is devoted to present the main ideas about the extension of the framework described in the previous sections to the nonlinear case. We still consider the system of equations (2.1)–(2.7), but now, instead of the Hooke's law (2.8), we suppose the following nonlinear constitutive law, called the Henky-von Mises law (cf. Nečas & Hlaváček (1981); Nečas (1986)):

$$\boldsymbol{\sigma}(\boldsymbol{u}) := [\kappa - \mu(\operatorname{dev}\boldsymbol{\varepsilon}(\boldsymbol{u}))]\operatorname{tr}\boldsymbol{\varepsilon}(\boldsymbol{u})\boldsymbol{I} + 2\mu(\operatorname{dev}\boldsymbol{\varepsilon}(\boldsymbol{u}))\boldsymbol{\varepsilon}(\boldsymbol{u}),$$

where, for $\boldsymbol{\tau} \in \mathbb{R}^{N\times N}$,

$$\operatorname{dev}\boldsymbol{\tau} := \left(\boldsymbol{\tau} - \frac{1}{2}\operatorname{tr}(\boldsymbol{\tau})\boldsymbol{I}\right) : \left(\boldsymbol{\tau} - \frac{1}{2}\operatorname{tr}(\boldsymbol{\tau})\boldsymbol{I}\right).$$

Here, κ is a positive constant, called the bulk modulus, and $\mu : \mathbb{R}^+ \to \mathbb{R}$ is a nonlinear Lamé function. We assume that $\mu \in \mathscr{C}^1(\mathbb{R}^+)$ and that there exist constants μ_1, μ_2 such that

$$0 < \mu_1 \leqslant \mu_1(t) < \kappa \quad \text{and} \quad 0 < \mu_1 \leqslant \mu(t) + 2t\mu'(t) \leqslant \mu_2,$$

for all $t \in \mathbb{R}^+$.

On the other hand, we will only consider the case in which the fluid is incompressible, i.e., $d(p,q) = 0$. The compressible case deserves further investigation since the theoretical results available for nonlinear problems with constraints (cf. Scheurer (1977)) do not apply to this situation.

Let $\mathscr{X}'$ be the dual space of $\mathscr{X}$ and let $\langle\cdot,\cdot\rangle$ be the duality paring on $\mathscr{X}' \times \mathscr{X}$. We define the mapping $\boldsymbol{A} : \mathscr{X} \to \mathscr{X}'$ by

$$\begin{aligned}\langle \boldsymbol{A}(\boldsymbol{u},\varphi),(\boldsymbol{v},\psi)\rangle &= \int_{\Omega_S} \boldsymbol{\sigma}(\boldsymbol{u}) : \boldsymbol{\varepsilon}(\boldsymbol{v}) \\ &= \int_{\Omega_S} \{[\kappa - \mu(\operatorname{dev}\boldsymbol{\varepsilon}(\boldsymbol{u}))]\operatorname{tr}\boldsymbol{\varepsilon}(\boldsymbol{u})\operatorname{tr}\boldsymbol{\varepsilon}(\boldsymbol{v}) + 2\mu(\operatorname{dev}\boldsymbol{\varepsilon}(\boldsymbol{u}))\boldsymbol{\varepsilon}(\boldsymbol{u}) : \boldsymbol{\varepsilon}(\boldsymbol{v})\}. \qquad \text{(A.1)}\end{aligned}$$

Using this mapping, the weak formulation of the problem is obtained by repeating exactly the same steps from the linear problem and we arrive at:

Find $((\boldsymbol{u},\varphi),p) \in \mathscr{X} \times \mathscr{M}$ such that

$$\langle \boldsymbol{A}(\boldsymbol{u},\varphi),(\boldsymbol{v},\psi)\rangle + b((\boldsymbol{v},\psi),p) = \boldsymbol{F}(\boldsymbol{v},\psi), \qquad \text{(A.2)}$$

$$b((\boldsymbol{u},\varphi),q) = 0, \qquad \text{(A.3)}$$

for all $((\boldsymbol{v},\psi),q) \in \mathscr{X} \times \mathscr{M}$.

Also, we propose a finite element scheme analogous to (3.1)–(3.2):

Find $((\boldsymbol{u}_h,\varphi_h),p_h) \in \mathscr{X}_h \times \mathscr{M}_h$ such that

$$\langle \boldsymbol{A}(\boldsymbol{u}_h,\varphi_h),(\boldsymbol{v}_h,\psi_h)\rangle + b((\boldsymbol{v}_h,\psi_h),p_h) = \boldsymbol{F}(\boldsymbol{v}_h,\psi_h), \qquad \text{(A.4)}$$

$$b((\boldsymbol{u}_h,\varphi_h),q_h) = 0, \qquad \text{(A.5)}$$

for all $((\boldsymbol{v}_h,\psi_h),q_h) \in \mathscr{X}_h \times \mathscr{M}_h$.

THEOREM A.1 The nonlinear mapping $\boldsymbol{A}$ defined in (A.1) defines a Lipschitz continuous operator, strongly monotone in $\mathscr{X} \cup \mathscr{X}_h$; namely, there exist strictly positive constants M and $\tilde{\alpha}$, independent of h, such that

$$\|\boldsymbol{A}(\boldsymbol{u},\varphi) - \boldsymbol{A}(\boldsymbol{v},\psi)\|_{\mathscr{X}'} \leqslant \mathscr{M}\,\|(\boldsymbol{u},\varphi) - (\boldsymbol{v},\psi)\|_{\mathscr{X}}$$

for all $(\boldsymbol{u},\varphi),(\boldsymbol{v},\psi)\in\mathscr{X}$ and

$$\langle \boldsymbol{A}(\boldsymbol{u},\varphi)-\boldsymbol{A}(\boldsymbol{v},\psi),(\boldsymbol{u},\varphi)-(\boldsymbol{v},\psi)\rangle \geqslant \tilde{\alpha}\,\|(\boldsymbol{u},\varphi)-(\boldsymbol{v},\psi)\|_{\mathscr{X}}^2$$

for all $(\boldsymbol{u},\varphi),(\boldsymbol{v},\psi)\in\mathscr{X}\cup\mathscr{X}_h$.

Proof. Following Gatica & Wendland (1997) we may prove:

$$\langle \boldsymbol{A}(\boldsymbol{u},\varphi)-\boldsymbol{A}(\boldsymbol{v},\psi),(\boldsymbol{u},\varphi)-(\boldsymbol{v},\psi)\rangle \geqslant \tilde{\alpha}\,\|\boldsymbol{u}-\boldsymbol{v}\|_{1,\Omega_S}^2,$$
$$\|\boldsymbol{A}(\boldsymbol{u},\varphi)-\boldsymbol{A}(\boldsymbol{v},\psi)\|_{\mathscr{X}'} \leqslant \mathscr{M}\,\|\boldsymbol{u}-\boldsymbol{v}\|_{1,\Omega_S},$$

for all $(\boldsymbol{u},\varphi),(\boldsymbol{v},\psi)\in\mathscr{X}$. Hence, we proceed as in the proofs of Lemmas 2.1 and 3.1 to conclude the theorem. □

THEOREM A.2 There exist unique solutions $((\boldsymbol{u},\varphi),p)$ and $((\boldsymbol{u}_h,\varphi_h),p_h)$ of problems (A.2)–(A.3) and (A.4)–(A.5), respectively. Moreover, there exists a constant $C>0$, independent of h, such that

$$\|\boldsymbol{u}-\boldsymbol{u}_h\|_{1,\Omega_S}+|\varphi-\varphi_h|_{1,\Omega_F}+\|p-p_h\|_{1,\Omega_F} \leqslant C\left(\inf_{\boldsymbol{v}_h\in\mathscr{H}_h}\|\boldsymbol{u}-\boldsymbol{v}_h\|_{1,\Omega_S}+\inf_{\psi_h\in\mathscr{V}_h}|\varphi-\psi_h|_{1,\Omega_F}+\inf_{q_h\in\mathscr{M}_h}\|p-q_h\|_{1,\Omega_F}\right).$$

Proof. It is enough to apply the previous theorem, Lemmas 2.2 and 3.2 and (Scheurer, 1977, Theorems 1.2 & 2.1) to conclude the existence and uniqueness of solution of both problems, (A.2)–(A.3) and (A.4)–(A.5), as well as the error estimate. □

Acknowledgments

The authors thank Pablo Gamallo and Luis Hervella-Nieto for providing a code which was used as a starting point for the computations. Rodolfo Araya has been partially supported by CONICYT through FONDECYT grant 1070698 and FONDAP and BASAL projects CMM, Universidad de Chile. Gabriel Barrenechea has been partially funded by Starter's Grant, Faculty of Sciences, University of Strathclyde. Fabrice Jaillet has been partially supported by Fundación Andes grant C-14055. Rodolfo Rodríguez has been partially supported by FONDAP and BASAL projects CMM, Universidad de Chile.

REFERENCES

BERMÚDEZ, A., GAMALLO, P., HERVELLA-NIETO, L., RODRÍGUEZ, R. & SANTAMARINA, D. (2008) Fluid-Structure Acoustic Interaction. *Computational Acoustics of Noise Propagation in Fluids.* (Marburg S. & Nolte B., eds.) Berlin, Heidelberg: Springer-Verlag, pp. 253–286.

BERMÚDEZ, A., GAMALLO, P., HERVELLA-NIETO, L. & RODRÍGUEZ, R. (2003) Finite element analysis of pressure formulation of the elastoacoustic problem. *Numer. Math.*, **95**, 29–51.

BRAESS, D. & BLÖMER, C. (1990) A multigrid method for a parameter dependent problem in solid mechanics. *Numer. Math.*, **57**, 747–761.

BRENNER, S. & SCOTT, L.R. (1994) *The Mathematical Theory of Finite Element Methods.* New York: Springer-Verlag.

BREZZI, F. & FORTIN, M. (1991) *Mixed and Hybrid Finite Element Methods.* New York: Springer-Verlag.

BUCHOLZ, R.D., YEH, D.D., TROBAUGH, J, MCDURMONT, L.L., STURM, C.D., BAUMANN, C., HENDERSON, J.M., LEVY, A. & KESSMAN, P. (1997) The correction of stereotactic inaccuracy caused by brain shift using an intraoperative ultrasound device. *CVRMed-MRCAS'97 First Joint Conference Computer Vision, Virtual Reality and Robotics in Medicine and Medical Robotics and Computer-Assisted Surgery.* (Troccaz, J. *et al.*, eds.) *Lecture Notes in Computer Science*, Vol. 1205.

ERN, A. & GUERMOND, J.-L. (2004) *Theory and Practice of Finite Elements.* New York: Springer-Verlag.

FUNG, Y.C. (1993) *Biomechanics: Mechanical Properties of Living Tissues.* New York: Springer-Verlag.

GASTALDI, L. (1996) Mixed finite element methods in fluid structure systems. *Numer. Math.*, **74**, 153–176.

GATICA, G.N. & WENDLAND, W. (1997) Coupling of mixed finite elements and boundary elements for a hyperelastic interface problem. *SIAM J. Numer. Anal.*, **34**, 2335–2356.

GRISVARD, P. (1985) *Elliptic Problems in Nonsmooth Domains.* Boston: Pitman.

HAGEMANN, A. (2001) *Biomechanical Model of the Human Head with Variable Material Properties for Intraoperative Image Correction.* Berlin: Logos.

HAGEMANN, A., ROHR, K. & STIEHL, H.S. (2002) Coupling of fluid and elastic models for biomechanical simulations of brain deformations using FEM. *Medical Image Analysis,* **6**, 375–388.

HAGEMANN, A., ROHR, K., STIEHL, H.S., SPETZGER, U. & GILSBACH, J.M. Nonrigid matching of tomographic images based on a biomechanical model of the human head. *Medical Imaging 1999 – Image Processing (MI'99).* (Hanson, K.M., ed.) *Proceedings of SPIE*, Vol. 3661, pp. 583–592.

HILL, D.L.G., MAURER, C.R., MACIUNAS, R.J., BARWISE, J.A., FITZPATRICK, J.M. & WANG, M.Y. (1998) Measurement of intraoperative brain surface deformation under a craniotomy. *Neurosurgery,* **43**, 514–526.

MAURER, C.R., HILL, D.L.G., MARTIN, A.J., LIU, H., MCCUE, M., RUECKERT, D., LLORET, D., HALL, W.A., MAXWELL, R.E., HAWKES, D.J. & TRUWIT, C.L. (1998) Investigation of intraoperative brain deformation using a 1.5-T interventional MR system: Preliminary results. *IEEE Transactions on Medical Imaging,* **17**, 817–825.

MORAND, H.-P. & OHAYON, R. (1995) *Fluid Structure Interaction.* Chichester: John Wiley & Sons.

NEČAS, J. (1986) *Introduction to the Theory of Nonlinear Elliptic Equations.* Chichester: John Wiley & Sons.

NEČAS, J. & HLAVÁČEK, I. (1981) *Mathematical Theory of Elastic and Elasto-Plastic Bodies: An Introduction.* Amsterdam-New York: Elsevier.

PAULSEN, K.D., MIGA, M.I., KENNEDY, F.E., HOOPES, P.J., HARTOV, A. & ROBERTS, D.W. (1999) A computational model for tracking subsurface tissue deformation during stereotactic neurosurgery. *IEEE Transactions on Biomedical Engineering*, **46**, 213–225.

SCHEURER, B. (1977) Existence et approximation de points selles pour certains problèmes non linéaires. *RAIRO Anal. Numér.*, **11**, 369–400.

SCOTT, L.R. & ZHANG, S. (1990) Finite element interpolation of nonsmooth functions satisfying boundary conditions. *Math. Comp.*, **54**, 483–493.

SHEWCHUCK, J. (2002) Delaunay refinement algorithms for triangular mesh generation. *Comp. Geom. Theor. Appl.*, **22**, 21–74.

VERFÜRTH, R. (1996) *A Review of A Posteriori Error Estimation and Adaptive Mesh-Refinement Techniques.* Chichester: John Wiley & Sons.

VERFÜRTH, R. (1998) A posteriori error estimators for convection-diffusion equations. *Numer. Math.*, **80**, 641–663.